



The Influence of Environmental Variability on the Biogeography of Coccolithophores and Diatoms in the Great Calcite Belt

Helen E. K. Smith^{1,2}, Alex J. Poulton^{1,3}, Rebecca Garley⁴, Jason Hopkins⁵, Laura C. Lubelczyk⁵, Dave T. Drapeau⁵, Sara Rauschenberg⁵, Ben S. Twining⁵, Nicholas R. Bates^{2,4}, William M. Balch⁵

¹National Oceanography Centre, European Way, Southampton, SO14 3ZH, U.K.

²School of Ocean and Earth Science, National Oceanography Centre Southampton, University of Southampton Waterfront Campus, European Way, Southampton, SO14 3ZH, U.K.

³Present address: The Lyell Centre, Heriot-Watt University, Edinburgh, EH14 7JG, U.K.

⁴Bermuda Institute of Ocean Sciences, 17 Biological Station, Ferry Reach, St. George's GE 01, Bermuda.

⁵Bigelow Laboratory for Ocean Sciences, 60 Bigelow Drive, P.O. Box 380, East Boothbay, Maine 04544, USA.

Correspondence to: Helen E.K. Smith (helen.eksmith@gmail.com)

Abstract. The Great Calcite Belt (GCB) of the Southern Ocean is a region of elevated summertime upper ocean calcite concentration derived from coccolithophores, despite the region being known for its diatom predominance. The overlap of two major phytoplankton groups, coccolithophores and diatoms, in the dynamic frontal systems characteristic of this region, provides an ideal setting to study environmental influences on the distribution of different species within these taxonomic groups. Water samples for phytoplankton enumeration were collected from the upper 30 m during two cruises, the first to the South Atlantic sector (Jan-Feb 2011; 60° W-15° E and 36-60° S) and the second in the South Indian sector (Feb-Mar 2012; 40-120° E and 36-60° S). The species composition of coccolithophores and diatoms was examined using scanning electron microscopy at 27 stations across the Sub-Tropical, Polar, and Sub-Antarctic Fronts. The influence of environmental parameters, such as sea-surface temperature (SST), salinity, carbonate chemistry (i.e., pH, partial pressure of CO₂ (*p*CO₂), alkalinity, dissolved inorganic carbon), macro-nutrients (i.e., nitrate+nitrite, phosphate, silicic acid, ammonia), and mixed layer average irradiance, on species composition across the GCB, was assessed statistically. Nanophytoplankton (cells 2-20 μm) were the numerically abundant size group of biomineralizing phytoplankton across the GCB, the coccolithophore *Emiliana huxleyi* and the diatoms *Fragilariopsis nana*, *F. pseudonana* and *Pseudonitzschia* sp. were the most dominant and widely distributed species. A combination of SST, macro-nutrient concentrations and *p*CO₂ were the best statistical descriptors of biogeographic variability of biomineralizing species composition between stations. *Emiliana huxleyi* occurred in the silicic acid-depleted waters between the Sub-Antarctic Front and the Polar Front, indicating a favorable environment for this coccolithophore in the GCB after spring diatom blooms remove silicic acid to limiting levels. After full consideration of variability in carbonate chemistry and temperature on the distribution of nanoplankton in the GCB, we find that temperature remains the dominant driver of biogeography in a large proportion of the modern Southern Ocean.



1 Introduction

The Great Calcite Belt (GCB), defined as an elevated particulate inorganic carbon (PIC) feature occurring in austral spring and summer in the Southern Ocean (Balch et al., 2005), plays an important role in climate fluctuations (Sarmiento et al. 1998, 2004), accounting for over 60% of the Southern Ocean area (30-60°S; Balch et al., 2011). The region between 30-50°S is recognized as having the highest uptake of anthropogenic carbon dioxide (CO₂) alongside the North Atlantic Ocean (Sabine et al., 2004). The impact of future perturbations of ocean chemistry on Southern Ocean phytoplankton biogeography (e.g., Passow and Carlson, 2012) is poorly constrained. Understanding the current environmental influences on phytoplankton biogeography is therefore critical if model parameterizations are to improve (Boyd and Newton, 1999) and provide more accurate predictions of future biogeochemical change.

The Southern Ocean has often been considered as a micro-plankton (20-200 µm) dominated system with phytoplankton blooms dominated by large diatoms and *Phaeocystis* sp. (e.g., Bathmann et al., 1997; Poulton et al., 2007; Boyd, 2002). However, since the recent identification of the GCB as a consistent feature (Balch et al., 2005; 2016) and the recognition of the importance of pico- (< 2 µm) and nanoplankton (2-20 µm) in High Nutrient Low Chlorophyll (HNLC) waters (Barber and Hiscock, 2006), the dynamics of small mineralizing plankton and their subsequent export need to be reconsidered. The two dominant mineralizing phytoplankton groups in the GCB are coccolithophores and diatoms. Coccolithophores are generally found north of the PF (e.g., Mohan et al., 2008), though *Emiliania huxleyi* has been observed as far south as 58°S in the Scotia Sea (Holligan et al., 2010), at 61°S across Drake Passage (Charalampopoulou et al., 2016) and 65°S south of Australia (Cubillos et al., 2007).

Diatoms are present throughout the GCB, with the Polar Front marking a strong divide between different size fractions (Froneman et al., 1995). North of the PF, small diatom species (< 20 µm) such as *Pseudonitzschia* sp. and *Thalassiosira* sp. tend to dominate numerically, whereas large diatoms (> 20 µm) with higher silicic acid requirements (e.g. *Fragilariopsis kerguelensis*) are generally more abundant south of the PF (Froneman et al., 1995). High abundances of nanoplankton (coccolithophores, small diatoms, chrysophytes) have also been observed on the Patagonian shelf (Poulton et al., 2013) and in the Scotia Sea (Hinz et al., 2012). Currently, few studies incorporate small mineralizing phytoplankton to species level (e.g., Froneman et al., 1995; Bathmann et al., 1997; Poulton et al., 2007; Hinz et al., 2012). Rather, the focus has often been on the larger and non-calcifying species of phytoplankton in the Southern Ocean due to sample preservation issues (i.e., acidified Lugol's solution dissolves calcite and light microscopy restricts accurate identification to cells > 10 µm; Hinz et al., 2012). The distribution of mineralizing phytoplankton is important to define when considering phytoplankton interactions with carbonate chemistry (e.g., Langer et al., 2006; Tortell et al., 2008) and ocean biogeochemistry (e.g., Baines et al., 2010; Assmy et al., 2013; Poulton et al., 2013).



The GCB begins south of $\sim 30^{\circ}$ S and extends to $\sim 60^{\circ}$ S covering an area of $\sim 88 \times 10^6$ km² (Balch et al., 2011), spanning the major Southern Ocean circumpolar fronts (Fig. 1a): the Sub-Antarctic front (SAF); the Polar Front (PF); the Southern Antarctic Circumpolar Current Front (SACCF); and occasionally, the Southern Boundary of the Antarctic Circumpolar Current (ACC, see Tsuchiya et al., 1994; Orsi et al., 1995; Belkin and Gordon, 1996). The Subtropical Front (STF; at approximately 10° C) acts as the northern boundary of the GCB and is associated with a sharp increase in PIC southwards (Balch et al., 2011). These fronts divide distinct environmental and biogeochemical zones making the GCB an ideal study area to examine the controls on phytoplankton communities in the open ocean (Boyd, 2002; Boyd et al., 2010). High PIC concentration observed in the GCB ($1 \mu\text{mol PIC L}^{-1}$) compared to the global average ($0.2 \mu\text{mol PIC L}^{-1}$) and significant quantities of detached coccoliths of the ubiquitous coccolithophore *Emiliania huxleyi* (in concentrations $> 20,000$ coccoliths mL⁻¹; Balch et al., 2011) both characterize the GCB. The GCB is clearly observed in satellite imagery (e.g.; Balch et al., 2005; Fig. 1b); spanning from the Patagonian Shelf (Signorini et al., 2006; Painter et al., 2010), across the Atlantic, Indian and Pacific Oceans and completes the Antarctic circumnavigation via the Drake Passage.

The waters of the GCB have been more specifically characterized as High Nitrate Low Silicate Low Chlorophyll (HNLSiLC; e.g., Dugdale et al., 1995; Leblanc et al., 2005; Moore et al., 2007; Le Moigne et al., 2013), where dissolved iron (dFe) is considered an important control on microplankton ($>20 \mu\text{m}$) growth (e.g., Martin et al., 1990; Gall et al., 2001; Venables and Moore, 2010). Sea-surface temperature (SST) gradients have long been recognized as a driving factor behind phytoplankton biogeography and community composition (Raven and Geider, 1988; Boyd et al., 2010). The influence of environmental gradients on mineralizing phytoplankton in the Scotia Sea and Drake Passage has also been assessed (Hinz et al., 2012; Charalampopoulou et al., 2016). However, the controls on the distribution of the mineralizing nanoplankton are yet to be established for the wider Southern Ocean and GCB. Previous studies have predominantly focused on a single environmental factor (Eynaud et al., 1999) or combinations of temperature, light, macronutrients and dFe (Poulton et al., 2007; Mohan et al., 2008; Balch et al., 2016) to explain phytoplankton distribution. The inclusion of carbonate chemistry as an influence on phytoplankton biogeography is a relatively recent development (e.g., Charalampopoulou et al., 2011, 2016; Hinz et al., 2012; Poulton et al., 2014; Marañón et al., 2016). Furthermore, natural variability in ocean carbonate chemistry and the resulting impacts on in situ phytoplankton populations remain one of the greatest biogeochemical uncertainties.

Increasing concentration of dissolved CO₂ in the oceans is resulting in 'ocean acidification' via a decrease in ocean pH (Caldeira and Wickett, 2003). In the high latitudes, where colder waters enhance the solubility of CO₂ and reduce the saturation state of calcite, there may be potential detrimental effects on calcifying phytoplankton (Doney et al., 2009). However, this may be species- (Langer et al., 2006) or even strain-specific (Langer et al., 2011), showing an optimum-response when the opposing influences of pH and bicarbonate are considered in a substrate-inhibitor concept (Bach et al., 2015). The response of non-calcifiers (e.g., diatoms) to ocean acidification is a greater unknown but no less important given their ~ 40 to 50% contribution to global primary production (e.g., Tréguer et al., 1995; Sarthou et al., 2005). Tortell et al.



(2008) observed a switch from small to large diatom species with increasing CO₂, indicating a potential change in future community structure. Large phytoplankton species (>50 μm) may also have the existing physiological traits to withstand changes in ocean chemistry over smaller (<50 μm) celled species (Flynn et al., 2012), as well as potentially being less susceptible to grazing pressure (Assmy et al., 2013). Alternatively, there may be a shift towards small phytoplankton groups due to the expansion of low-nutrient subtropical regions (Bopp et al., 2001; Bopp, 2005). The response of Southern Ocean phytoplankton biogeography to future climate conditions, including ocean acidification, is complex (e.g., Charalampopolou et al., 2016; Petrou et al., 2016; Deppeler and Davidson, 2017) and therefore understanding existing relationships between *in situ* phytoplankton communities and ocean chemistry is an important stepping-stone for predicting future changes.

Here, we assess the distribution of coccolithophore and diatom species in relation to the environmental conditions encountered across the GCB. Diatom and coccolithophore cell abundances were obtained from analysis of scanning electron microscopy (SEM) images, and their distribution statistically assessed in relation to SST, salinity, mixed layer average irradiance, macronutrients and carbonate chemistry. Herein, we examine the spatial differences within the mineralizing phytoplankton in the GCB, the main environmental drivers behind their biogeographic variability and the potential effects of future carbonate chemistry perturbations.

2 Methods

2.1 Sampling area

Two cruises were undertaken in the GCB during 2011 and 2012 (<http://www.bco-dmo.org/project/473206>). The Atlantic sector of the Southern Ocean (GCB1) was sampled from 11th January to 16th February 2011 onboard the R/V *Melville*, between Punta Arenas, Chile and Cape Town, South Africa (Balch et al., 2016; Fig. 1). The Indian sector of the Southern Ocean (GCB2) was sampled from 18th February to 20th March 2012 onboard the R/V *Revelle* between Durban, South Africa and Fremantle, Australia (Fig. 1). Water samples were taken at 27 stations across a latitudinal gradient ranging from 38° S to 60° S and a longitudinal gradient ranging from 60° W to 120° E during the GCB cruises, which enabled sampling of the major oceanographic features of this region.

2.1 Physiochemical environmental conditions

Water samples, for this study, were collected from the upper 30 m of the water column using a Niskin bottle rosette and CTD profiler for sea surface temperature, salinity, chlorophyll *a* (Chl *a*), nitrate plus nitrite (TOxN), ammonia (NH₄), phosphate (PO₄), silicic acid (Si(OH₄)), and carbonate chemistry. Nutrient analyses of TOxN, PO₄, Si(OH₄) and NH₄ were run on a Seal Analytical continuous-flow AutoAnalyzer 3, while salinity was determined using a single Guildline Autosol 8400B stock salinometer (S/N 69-180). Chlorophyll *a* was sampled in triplicate following Joint Global Ocean Flux Studies (JGOFS; Knap. et al, 1996) protocols. Mixed layer depths were calculated from processed CTD data applying a criteria of a



0.02 kg m⁻³ density change from the 5 m depth value (Arrigo et al., 1998). Daily surface Photosynthetically Active Radiation (PAR) irradiance (mol PAR m⁻² d⁻¹) was estimated from eight-day composite Aqua MODIS data from the closest time and latitude-longitude point (averages were taken where necessary). Mixed layer average irradiance (\bar{E}_{MLD}) was calculated from the daily PAR following Poulton et al. (2011).

- 5 Water samples were collected for dissolved inorganic carbon (C_T) and Total Alkalinity (A_T) following standardized methods and analyzed using a Versatile Instrument for the Determination of Titration Alkalinity (VINDTA) with precision and accuracy of $\pm 1 \mu\text{mol kg}^{-1}$ (Bates et al., 1996; Bates et al., 2012). The remaining carbonate chemistry parameters were calculated from the C_T and A_T values using CO2SYS (Lewis and Wallace, 1998) and CO2calc (Robbins et al., 2010) with the carbonic acid dissociation constants of Mehrbach et al. (1973) refitted by Dickson and Millero (1987). This includes
- 10 computation of the saturation state (Ω) for calcite (i.e., Ω_{calcite}).

2.2 Phytoplankton enumeration

Samples for mineralizing phytoplankton community structure were also taken from the upper 30 m of the water column. At each sampling station 1 L seawater samples were collected and pre-filtered through a 200 μm mesh to remove any large zooplankton. Seawater samples were then gently filtered through a 25 mm, 0.8 μm Whatman® polycarbonate filter with a

15 200 μm mesh as a backing filter to ensure an even distribution of cells across the filter. The filters were rinsed with $\sim 5 \text{ mL}$ potassium tetraborate (0.02 M) buffer solution (pH = 8.5) to prevent salt crystal growth and PIC dissolution, air dried and stored in petri slides in the dark with a desiccant until further analysis.

To identify coccolithophores to the species level, each sample was imaged using the SEM methodology of Charalampopoulou et al. (2011). A central portion of each filter was cut-out, gold-coated and 225 photographs were taken at

20 a magnification of 5000x (equivalent to $\sim 1 \text{ mm}^2$; GCB1) or 3000x ($\sim 2.5 \text{ mm}^2$; GCB2) using a Leo 1450VP SEM (Carl Zeiss, Germany). Detached coccoliths and whole coccolithophore cells (coccospheres) were identified following Young et al. (2003). Diatoms and other recognizable protists were identified following Hasle and Syvertsen (1997) and Scott and Marchant (2005). Where a confident species level identification was not possible, cells were assigned to the level of genera (e.g., *Chaetoceros* sp. or *Pappamonas* sp.). Each species identified was enumerated using the freeware ImageJ (v1.44o) for

25 all 225 images or until 300 cells (or coccoliths) were counted. A minimum of 10 random images was picked for enumeration when species were in high abundance ($> 1000 \text{ cells mL}^{-1}$). The abundance of each species was calculated following Eq. (1):

$$\text{Cells mL}^{-1} = (C \times F/A)/V \quad (1)$$

where C is the total number of cells (or coccoliths) counted, A is the area investigated (mm^2), F is the total filter area (mm^2)

30 and V is the volume filtered (mL).



2.3 Statistical analysis

Multivariate statistics (PRIMER-E v.6.1.6; Clarke and Gorley, 2006) were used to examine spatial changes in coccolithophore and diatom abundance, species distribution and the influence of environmental variability on biogeography (e.g., Charalampopoulou et al., 2011, 2016). Environmental data was initially assessed for skewness, most likely due to strong chemical gradients across fronts. Heavily left-skewed variables (TOxN, silicic acid and NH₄) were log(V+0.1) transformed to reduce skewness and stabilize variance. Other environmental data, including SST, salinity, \bar{E}_{MLD} , TOxN, silicic acid, NH₄, pH, pCO_2 and $\Omega_{calcite}$ was then normalized to a mean of zero and a standard deviation of one, and Euclidean distance was then used to determine spatial changes. A principal component analysis (PCA) was used to simplify environmental variability, by combining the more closely correlated variables and the relative influence of the environmental variables within the data (Clarke, 1993; Clarke and Warwick, 2001; Clarke and Gorley, 2006).

Coccolithophore and diatom species diversity was assessed as the total number of species (S), and Pielou's evenness index (J') which assesses how evenly the count data was distributed between the different species present. Species with cell counts of less than 1 cell mL⁻¹, and/or consistently representing less than 1% of the total cell abundance, were excluded from multivariate statistical analysis to reduce the influence of rare species. Analysis of coccolithophore and diatom community structure was carried out on standardized and square root transformed cell abundance (to reduce the influence of numerically abundant species) using a Bray-Curtis similarity matrix. To identify which stations had a statistically similar plankton community across the GCB a SIMPROF routine (1000 permutations, 5% significance level) was applied to the Bray-Curtis similarity matrix. The phytoplankton species driving the differences between the groups were identified through a SIMPER routine and presented using non-metric multidimensional scaling (nMDS; Clarke, 1993; Clarke and Warwick, 2001; Clarke and Gorley, 2006).

A BEST routine was applied to environmental and plankton data to determine the combination of environmental variables that 'best' described the variability in coccolithophores and diatoms across the GCB. Spearman's rank correlations were used to further investigate the relationship between key environmental variables identified in the BEST routine and selected coccolithophore and diatom species.

25 3 Results

3.1 General Oceanography

The GCB cruises crossed various biogeochemical gradients associated with the Antarctic Circumpolar Current (ACC) fronts and currents, with most parameters following a recognizable latitudinal (or zonal) pattern. The position of oceanic fronts referred to in the following text relates to those defined in Fig. 1 (see also Balch et al., 2016). Sea-surface temperature decreased southwards from 21° C north of the STF to 1.1° C close to 60° S (Table 1). Calcite saturation state ($\Omega_{calcite}$)



decreased from 5.2 north of the subtropical front to 2.6 close to 60° S (Table 1). Macronutrient concentrations generally increased southwards with a distinct divide across the SAF. TOxN ranged from below detection limits ($<0.1 \mu\text{mol L}^{-1}$) to as high as $28 \mu\text{mol L}^{-1}$, with higher concentrations generally south of the Sub-Antarctic Front ($>12 \mu\text{mol L}^{-1}$), and lower concentrations ($<7 \mu\text{mol L}^{-1}$) north of the Sub-Antarctic Front (Table 1). PO_4 followed a very similar pattern with concentrations generally greater than $1 \mu\text{mol L}^{-1}$ south of the Sub-Antarctic Front and $<0.6 \mu\text{mol L}^{-1}$ to the north. Silicic acid concentrations were divided by the PF, being generally less than $2 \mu\text{mol L}^{-1}$ to the north and up to $78.5 \mu\text{mol L}^{-1}$ to the south (Table 1). \bar{E}_{MLD} was highest on the Patagonian Shelf ($\sim 40 \text{ mol photons m}^{-2} \text{ d}^{-1}$) and generally less than $10 \text{ mol photons m}^{-2} \text{ d}^{-1}$ south of the Sub-Antarctic Front (Table 1). There was no distinct latitudinal trend in pH or $p\text{CO}_2$. Surface water pH was generally greater than 8.06, ranging from 8.03 on the Kerguelen plateau to 8.13 in the Sub-Tropical Front south-west of Australia (Table 1). Surface water $p\text{CO}_2$ ranged from 299 μatm to 444 μatm with both extremes in the vicinity of the Atlantic STF (Table 1). Chl *a* concentrations were variable across the oceanic gradients, highest on the Patagonian Shelf (2.78 mg m^{-3}) and on average less than 1 mg m^{-3} in the South Atlantic compared with less than 0.5 mg m^{-3} in the South Indian Ocean (Table 1).

3.2 Coccolithophores and diatoms

The most frequently occurring and abundant size group within the coccolithophores and diatoms were the nanoplankton (cells 2-20 μm). Large diatom species (cells $>20 \mu\text{m}$) were found in higher numbers (up to 50 cells mL^{-1}) south of the PF but were not numerically dominant compared to the nanoplankton species at these locations. Total cell abundances were less than $1000 \text{ cells mL}^{-1}$ at most stations (Table 2), which are indicative of late summer, non-bloom conditions. In the South Atlantic, the highest abundance of coccolithophores was on the Patagonian Shelf (station GCB1-16; $1,636 \text{ cells mL}^{-1}$) and the highest abundance of diatoms was east of the South Sandwich Islands (station GCB1-77; $6,787 \text{ cells mL}^{-1}$; Table 2). These were also the highest total abundances of coccolithophores and diatoms encountered across the entire GCB. In the South Indian Ocean, coccolithophore abundance was highest near the Crozet Islands (station GCB2-27; $472 \text{ cells mL}^{-1}$) and the diatom abundance was highest at the most southerly station (station GCB2-73; $514 \text{ cells mL}^{-1}$; Table 2). There were no stations in the South Indian Ocean with coccolithophore and diatom abundances were greater than $1,000 \text{ cells mL}^{-1}$ (Fig. 2, Table 2).

Coccolithophores dominated the mineralizing plankton community at twelve stations in terms of abundance north of the PF (Fig. 2, Table 2). On average coccolithophores contributed approximately 38% to total (coccolithophore and diatom) abundance in the GCB. Coccolithophores were greater than 75% of total abundance at only one station, north of South Georgia (station GCB1-59), and never accounted for 100% of total cell numbers. Twenty-eight species of coccolithophores were identified as intact coccospheres across the GCB. Coccolithophore diversity decreased south towards 60° S, with the highest coccolithophore diversity (13 species) found in the vicinity of the STF in the eastern part of the South Indian Ocean (station GCB2-106), while species contributions to total coccolithophore abundance was more evenly distributed between



the different species in the lower latitudes (i.e., high J' ; Table 2). *Emiliana huxleyi* was the most numerically abundant coccolithophore at all but four stations and was encountered in the mixed layer at all stations except one (station GCB2-73). Other coccolithophore species (e.g., *Syracosphaera* sp. and *Umbellosphaera* sp.) were present north of the PF throughout the GCB and were most abundant north of the STF. At stations south of the SAF (50° S) only one (*E. huxleyi*) or two species (*E.*
5 *huxleyi* and *Pappamonas* sp.) were observed as intact coccospheres.

Diatoms dominated 15 stations in terms of mineralizing plankton numerical abundance across all environments sampled (Fig. 2, Table 2) and were found in every sample analyzed, contributing 62% on average to the total cell (coccolithophores + diatoms) abundance. Diatoms made up 100% of the total cell counts at the most southerly station in the South Indian Ocean (station GCB2-73) and 99.7% east of the South Sandwich Islands (station GCB1-77; Fig. 2). Seventy-six species of diatom
10 were identified as intact cells across the entire GCB. The most frequently occurring species in the GCB were small (< 5 μm in length) *Fragilariopsis* ssp.. The highest abundance of diatoms in the South Atlantic Ocean (6,787 cells mL^{-1}) was dominated by *F. nana* east of the South Sandwich Islands (station GCB1-77). The highest diatom abundance in the South Indian Ocean (514 cells mL^{-1}) was dominated by *F. pseudonana* at the most southerly station (station GCB2-73) sampled. Another frequently dominant diatom was *Pseudonitzschia* sp. that was most abundant north of the PF (Table 2).

15 Diatom species richness increased south towards 60° S with the contribution of the different diatom species to total mineralizing plankton abundance fairly even ($J' > 0.5$, Table 2), except at stations (stations GCB1-70, GCB1-77, GCB2-27 and GCB2-63) where *Fragilariopsis* ssp. <5 μm were dominant (>70% of the diatom population, $J' < 0.5$). The highest diatom species richness (15 species) was found in the GCB south of the SAF (stations GCB1-85 and GCB2-36) at temperatures of 5°C to 8°C, in HNLSiLC conditions ($\text{TOxN} > 18 \mu\text{mol L}^{-1}$, silicic acid <2 $\mu\text{mol L}^{-1}$, Chl a 0.21-1.11 mg m^{-3}).

20 3.3 Statistical Analysis

Three of the environmental variables were removed from the statistical analysis following a Spearman's rank (r_s) correlation analysis (Table S1). TOxN and PO_4 had a strong significant positive correlation ($r_s = 0.961$, $p < 0.0001$) and so TOxN was deemed representative of both nutrients. Sea-surface temperature displayed significant negative correlations with both C_T ($r_s = -0.981$, $p < 0.0001$) and A_T ($r_s = -0.953$, $p < 0.0001$), and so sea surface temperature was taken as being representative of
25 these two variables of the carbonate chemistry system.

The variation in environmental variables across the GCB was examined using a Principal Component Analysis (PCA). The first principal component (PC1) accounted for 58% of the variation in environmental variables, with an additional 17% of environmental variation described by PC2 (Table 3). PC1 describes the main latitudinal gradients of environmental changes across the GCB (decreasing SST, increasing macronutrients). PC1 is a predominantly linear combination of SST, salinity,
30 TOxN , silicic acid, NH_4 , and Ω_{calcite} , where there is a significant positive correlation of PC1 with SST and salinity and a significant negative correlation with all other variables (Table 3). PC2 represented the environmental variation in the GCB



occurring independently of latitude, and was driven predominantly by variation in $p\text{CO}_2$, with weaker influences from \bar{E}_{MLD} and pH (Table 3). PC2 had significant positive correlations with $p\text{CO}_2$ and \bar{E}_{MLD} and a negative correlation with pH.

Variability in coccolithophore and diatom species composition across the GCB was assessed using a SIMPROF routine, comparing the abundance and diversity across all stations, to define groups with statistically similar community composition.

5 Six statistically significant groups ($p < 0.05$) were defined across the GCB (Fig. 3). Three groups of these groupings (A, B, C) were specific to the South Atlantic Ocean (Fig. 3). For example, groups A and B represented individual stations GCB1-46 and GCB1-117 respectively, in the sub-tropical region of the South Atlantic Ocean. The most southerly stations in the South Atlantic Ocean (stations GCB1-70 and GCB1-77) defined group C (Fig. 3). Groups D, E and F included stations across the GCB in both ocean regions. Here, group D was defined by eight stations sampled predominantly north of the SAF, while
10 group F was defined by 11 stations predominantly sampled south of the SAF (Fig. 3). These statistically defined similar community structures indicate that although the GCB covers a wide expanse of ocean, the community structure is consistently latitudinal defined across its longitudinal range.

The species driving the differences in mineralizing plankton community structure across the GCB were identified through a SIMPER routine (Table 4). Groups A and B were defined by the absence of *E. huxleyi* and the presence of either
15 holococcolithophores (group A) or the diatom *Cylindrotheca* sp. (group B). Group C was defined by the presence of *F. nana* (Table 4) and low contributions from *E. huxleyi* and *Pseudonitzschia* sp., with low diversity overall (total of 9 mineralizing species; Table 2) resulting in a significant difference from the other groups. Group D had higher total species diversity overall (i.e., 12-23 species; Table 2) and was defined by similar relative abundances of *E. huxleyi* and *Pseudonitzschia* sp., which were not found elsewhere (Table 4). Group E, including stations north of the SAF (Fig. 3), included *E. huxleyi*, *U.*
20 *tenuis* and holococcolithophores (Table 4). The low abundance of diatoms (3-125 cells mL^{-1} ; Table 2) within group E separated it from the other groups (Table 4). The combination of *E. huxleyi*, *F. pseudonana* and *Pseudonitzschia* sp. that defined group F (Table 4) represented stations on the Patagonian Shelf and south of the SAF (Fig. 3). The almost mono-specific *E. huxleyi* coccolithophore community (Table 2) in group F highlights its strong dissimilarity from the other community structure groups identified (Table 4).

25 The abundance and distribution of four nanophytoplankton species, *E. huxleyi*, *Pseudonitzschia* sp., *F. nana* and *F. pseudonana* (Fig. 4), were identified as having the most significant contribution to differences in community structure across the GCB (Table 4, Fig. 5). *Emiliania huxleyi* and *F. pseudonana* were the most dominant coccolithophore and diatom species, respectively, across the GCB (Table 2). *Fragilariopsis pseudonana* was the numerically dominant diatom (> 30%) at seven stations in the South Indian Ocean (Table 2). The diatom with the highest abundance, *F. nana* (6797 cells mL^{-1}),
30 was almost exclusively found in the South Atlantic Ocean (Table 2; Fig. 5) and the more frequently occurring *Pseudonitzschia* sp. was present at all but two stations (Fig. 5).



The influence of environmental variables on the biogeography of coccolithophores and diatoms in the GCB was assessed using the BEST routine. The strongest Spearman's rank correlation ($r_s = 0.55$, $p < 0.001$) between all possible environmental variables and the biogeographical patterns observed came from a combination of five variables, including: (1) SST; (2-4) macronutrients (TOxN, silicic acid, NH_4); and (5) $p\text{CO}_2$. This was followed by a correlation of $r_s = 0.54$ ($p < 0.001$) that included these parameters as well as Ω_{calcite} . Salinity was included in the third highest correlation, whereas \bar{E}_{MLD} and pH did not rank as significant factors in the BEST analysis.

4 Discussion

4.1 Biogeography of coccolithophores and diatoms in the Great Calcite Belt

Studies of Southern Ocean phytoplankton productivity have generally focused on the micro-phytoplankton (Barber and Hiscock, 2006) as these species contribute around 40% to total oceanic primary production (Tréguer et al., 1995; Sarthou et al., 2005). However, nanoplankton and picoplankton are becoming increasingly recognised as important contributors to total phytoplankton biomass, productivity and export in the Southern Ocean (e.g., Boyd, 2002; Hinz et al., 2012), both as the dominant size group in post-bloom (Le Moigne et al., 2013) and non-bloom conditions (Barber and Hiscock, 2006).

In this study, coccolithophores were generally numerically dominant at stations sampled north of the PF, particularly around the SubAntarctic Front, whereas diatoms were observed to be dominant at stations south of the PF (Fig. 2). There was also a significantly different species distribution (*a priori* ANOSIM; $R = 0.227$, $p < 0.01$) north and south of the Sub-Antarctic Front, which has been previously identified as the divider between calcite and opal dominated export in the Southern Ocean (e.g., Honjo et al., 2000; Balch et al., 2016). Diatoms were more abundant (~ 570 cells mL^{-1}) than coccolithophores (~ 160 cells mL^{-1}) on average in the entire GCB. This contrasts to a study by Eynaud et al. (1999) in the South Atlantic Ocean at a similar time of year that reported a peak in coccolithophore cell abundance in the vicinity of the PF (a feature that was not observed in this study). These differences are likely to be due to the variability of Southern Ocean plankton on short temporal scales (Mohan et al., 2008), including variability in the seasonal progression of the spring bloom (Bathmann et al., 1997).

The coccolithophore *E. huxleyi* and diatoms *F. pseudonana*, *F. nana* and *Pseudonitzschia* sp. (Fig. 4) were all identified as being central to defining the statistical similarities within, and the differences between, the different mineralizing phytoplankton groups (Table 4, Fig. 5). These four species are all part of the nanoplankton and at the lower end of the size range of the microplankton (*Pseudonitzschia* sp. is ~ 20 μm in length), which can contribute significantly to biomass in the HNLC regions of the Southern Ocean (Boyd, 2002). *Emiliania huxleyi* and *Fragilariopsis* sp. less than 10 μm have been identified as two of the most abundant mineralizing phytoplankton further south in the Scotia Sea (Hinz et al. 2012). The results presented here further indicate that nanoplankton do have the potential to contribute a significant proportion to GCB



community composition alongside the larger phytoplankton (including large diatoms) typically associated with the HNLC region.

The abundance of HNLC diatoms such as *F. kerguelensis* (<10 cells mL⁻¹), *T. nitzschoides* (<20 cells mL⁻¹) and large *Chaetoceros* sp. (<10 cells mL⁻¹) were generally lower than those observed in other studies (e.g., Poulton et al., 2007; Armand et al., 2008; Korb et al., 2010, 2012). Furthermore, the virtual absence of *Eucampia antarctica* (<1 cell mL⁻¹) in this study does not reflect the typical assemblage (sometimes > 600 cells mL⁻¹) found in previous studies (e.g., Kopczyaska et al., 1998; Eynaud et al., 1999; de Baar et al., 2005; Poulton et al., 2007; Salter et al., 2007; Korb et al., 2010). Low abundances of the large-celled diatoms in the silicic acid replete regions could be influenced by the small filter area analyzed using SEM; in this study the area imaged equates to a relatively small volume of water (i.e., 2-6 mL depending on magnification) relative to the larger volumes (10-50 mL) often examined for light microscopy in other studies. Large, rare cells may not be enumerated from such small sample volumes, however the numerically abundant nanoplankton groups were well represented in SEM images. Conversely, samples preserved in acidic Lugol's solution for light microscopy analysis are biased towards larger species since small diatoms (<10 µm) are not clearly visible and coccolithophores are not well preserved (Hinz et al., 2012). Therefore, in future a combination of both imaging techniques should be used when examining the phytoplankton community structure of the wider Southern Ocean.

4.2 *Emiliana huxleyi* in the Great Calcite Belt

The importance of coccolithophores in the GCB was examined via species community composition and abundance of intact cells, focusing on areas identified as having high PIC reflectance from underway sampling and satellite observations (Balch et al., 2014, 2016). Higher species diversity of coccolithophores occurred north of the STF (i.e., 4-13 species; Table 2). Coccolithophores are diverse in the stratified and low-nutrient waters associated with lower latitudes (Winter et al., 1994). Only a few species are found in the colder waters south of the STF (Mohan et al., 2008), the most successful being *E. huxleyi*, which was observed at an abundance of 103 cells mL⁻¹ at 1°C in this study in the South Atlantic (station GCB1-70). The 2°C isotherm has been previously assumed to represent the southern boundary of *E. huxleyi* (e.g., Verbeek, 1989; Mohan et al., 2008) and inter-annual variability could be influenced by movement of the southern front of the Antarctic Circumpolar Current (Holligan et al., 2010). The Southern Ocean *E. huxleyi* morphotype (Cook et al., 2011; Poulton et al., 2011) may therefore have a wider temperature tolerance than its northern hemisphere equivalent (Hinz et al., 2012) and has been observed poleward of 60° S further east in the Southern Ocean (Cubillos et al., 2007) and across Drake Passage (Charalampopoulou et al., 2016). There were three distinct *E. huxleyi* features (the Patagonian Shelf, north of South Georgia and north of the Crozet Islands) within the GCB where *E. huxleyi* contributed > 50% of the total cell counts of mineralizing phytoplankton. *Emiliana huxleyi* was most abundant (1636 cells mL⁻¹) on the Patagonian Shelf and was the most frequently occurring coccolithophore across the entire GCB. The main *E. huxleyi* features are discussed further below to understand why this species is so widely distributed in the GCB.



4.2.1 Patagonian Shelf

The Patagonian Shelf is a well-known region for *E. huxleyi* blooms, as observed in satellite imagery between November and January (i.e., Signorini et al., 2006; Painter et al., 2010; Balch et al., 2011; Garcia et al., 2011; Balch et al., 2014). The *E. huxleyi* cell abundance observed in this study (~ 1600 cells mL^{-1}) was similar to that found by Poulton et al. (2013; >1000 cells mL^{-1}). Using a value of 0.2 pg Chl *a* per cell (Haxo, 1985) following Poulton et al. (2013), such *E. huxleyi* abundance levels are equivalent to contributions of only $\sim 12\%$ to the total Chl *a* signal (~ 2.8 mg m^{-3}), which is a similar contribution to that estimated in an identical way by Poulton et al. (2013). This data combined with the satellite observations supports the hypothesis of a similar phytoplankton structure repeating on an inter-annual basis, although the contribution of *E. huxleyi* to net primary production may vary. The optimum range for *E. huxleyi* blooms on the Patagonian Shelf has been identified as between 5-15°C at depleted silicic acid levels relative to nitrate (Balch et al. 2014; 2016). During this study, silicic acid was drawn-down to undetectable levels on the Patagonian Shelf (Table 1), with the source water for this region being Southern Ocean HNLSiLC waters transported northwards via the Falklands current (Painter et al., 2010; Poulton et al., 2013). The persistent low silicic acid availability and residual nitrate (defined as $[\text{NO}_3^-] - [\text{Si}(\text{OH})_4]$) on the Patagonian Shelf is therefore an ideal environment for *E. huxleyi* to grow without the competition of large, fast growing diatoms (Balch et al., 2014).

15 4.2.2 South Georgia

South Georgia is renowned for intense diatom blooms of over 600 cells mL^{-1} with Chl *a* over 10 mg m^{-3} and integrated primary production up to 2 g C $\text{m}^{-2} \text{d}^{-1}$ (Korb et al., 2008). However, *E. huxleyi* was the dominant species ($>75\%$ of total cell numbers) within the diatom and coccolithophore population at the station north of South Georgia (Table 2, Fig. 2). The associated calcite feature can also be identified from the satellite composite in Fig. 1 (38° E, 51° S). *Emiliana huxleyi* contributed approximately 15% (using 0.2 pg Chl *a* per cell) to the total Chl *a* signal (0.71 mg m^{-3}) around South Georgia. The high calcite feature at South Georgia was found at SST of 5.9°C, which is below the considered 'optimum' growth conditions for *E. huxleyi* previously cultured (Paasche, 2001). This population of *E. huxleyi* was most likely an adapted cold water morphotype (Cook et al., 2011; Poulton et al., 2011; Cook et al., 2013). The dominant diatom species here was *Actinocyclus* sp. and highly silicified *Thalassionema nitzschoides* with silicic acid concentrations likely limiting (1.7 $\mu\text{mol Si L}^{-1}$; Paasche 1973a & b), whereas TOxN concentrations (17.5 $\mu\text{mol N L}^{-1}$) and PO_4 concentrations (1.22 $\mu\text{mol P L}^{-1}$) can be considered replete. The low silicate concentrations could explain why *Eucampia antarctica* was not observed in this study, but has been observed north of South Georgia previously (Korb et al., 2010, 2012). This indicates that preceding diatom growth event had depleted silicic acid (and other nutrients such as dissolved iron), allowing *E. huxleyi* to become more dominant in the population with a similar residual nitrate environment as found on the Patagonian Shelf (this study, Balch et al., 2014; Balch et al., 2016).



4.2.3 Crozet Islands

The *E. huxleyi* feature north of the Crozet Islands with an abundance of 472 cells mL⁻¹ (highest in the South Indian Ocean) confirms the presence of coccolithophores this region. Coccolithophore abundances have not previously been reported in this region, although elevated PIC had been observed and attributed to *E. huxleyi* (Read et al., 2007; Salter et al., 2007). Chl *a* was lowest (0.47 mg m⁻³) at Crozet out of all three high PIC features, though *E. huxleyi* contributed ~20% of this signal (based on 0.2 pg Chl-*a* per cell), proportionally higher than on the Patagonian Shelf and near South Georgia. Previous studies around the Crozet Islands and plateau (2004-2005) have found indications of coccolithophores in sediment trap samples (Salter et al. 2007) and associated large (>30 mmol C m⁻² d⁻¹) calcite fluxes (Le Moigne et al., 2012), though surface cell counts were unavailable (Read et al., 2007). The satellite-derived calcite signal was observed to increase after the main Chl *a* event in this study (Fig. S1) and in previous years (Salter et al., 2007). An increase in coccolithophore abundance following a diatom bloom is also observed in other oceanic regions from satellite-derived products (Hopkins et al., 2015) and is associated with depletion of dissolved iron and/or silicic acid (Holligan et al., 2010) in addition to a stable water column and increased irradiance (Balch et al., 2014).

4.2.4 Summary of biogeochemical characterization of coccolithophore occurrence and abundance

The Southern Ocean was previously considered to have a mineralizing phytoplankton community dominated by diatoms. This study highlights that *E. huxleyi* can form distinct features within the GCB and contribute up to 20% towards total Chl *a* in these features compared to an average of less than 5% Chl *a* across the rest of the GCB. Hence, *Emiliania huxleyi* is likely to have a more important role in biogeochemical processes in the GCB than previously thought. This is particularly important to consider when assessing the impact on calcium carbonate associated export (e.g., Honjo et al., 2000; Balch et al., 2010; Balch et al., 2016) in the Southern Ocean. If *E. huxleyi* is migrating poleward with time (Winter et al., 2013) then the dynamics of the carbon system in the GCB may change, particularly south of the SAF, where silicic acid derived export has historically been dominant (Honjo et al., 2000; Pondaven et al., 2000). Thus it is essential to gain an understanding of the environmental factors driving the distribution of *E. huxleyi* (Winter et al., 2013, Charalampopoulou et al., 2016) amongst other phytoplankton in the GCB to better predict the future biogeochemistry of the Southern Ocean.

4.3 Environmental controls on biogeography

The environmental variables that best describe coccolithophore and diatom species distribution in this study were SST, macronutrients (TOxN, silicic acid, NH₄) and *p*CO₂ (Spearman's rank correlation = 0.55, *p* < 0.001), with the second highest correlation (Spearman's rank correlation = 0.54, *p* < 0.001) including calcite saturation state (Ω_{calcite}). The inclusion of *p*CO₂ and Ω_{calcite} as important factors indicates a potential influence of carbonate chemistry on coccolithophore and diatom distribution (and *vice versa*) in the GCB. However, Ω_{calcite} had a very strong positive correlation (*r* = 0.964, *p* < 0.0001) with



SST (Table S1) and therefore separating the influences of the two variables was impossible in this study due to the tight coupling between carbonate chemistry and temperature (as also observed by Charalampopoulou et al., 2016).

4.3.1 Temperature

Temperature is recognized as a strong driving factor behind plankton biogeography and community composition (Raven and Geider, 1988; Boyd et al., 2010). The abundance of two of the dominant species *E. huxleyi* and *F. pseudonana* did not significantly correlate (Pearson's product moment correlation = 0.147, $p = 0.493$ and $r = -0.247$, $p = 0.357$ respectively) with SST, which does not agree with previous work (e.g., Mohan et al., 2008) and implies that *E. huxleyi* distribution is not solely determined by latitudinal variations in temperature. Nanoplankton are subject to high grazing pressure (Schmoker et al., 2013) and the growth and mortality of a species both directly influence cell abundances (Poulton et al., 2010), which could result in patchiness and deviation away from the theoretical species abundances relative to temperature or other environmental factors. In contrast, the negative correlation of *F. nana* (Pearson's product moment correlation = -0.976, $p < 0.05$, $n = 4$) versus the positive correlation of *Pseudonitzschia* sp. (Pearson's product moment correlation = 0.544, $p < 0.05$, $n = 19$) with SST indicates that these two species have distinctly different physiological tolerances. Southern Ocean diatoms are mostly observed to have negative relationship with temperature (e.g. Eynaud et al., 1999; Boyd, 2002). *Pseudonitzschia* sp. was predominantly found in waters north of the PF in this study, as seen by Kopczynska et al. (1986), and is likely to be out competed by other diatom species (e.g. *Chaetoceros* sp. and *Dactyliosolen* sp.) further south due to different nutrient affinities and requirements (Kopczynska et al., 1986), particularly for dissolved iron and silicic acid.

4.3.2 Nutrients

Macronutrient gradients, particularly silicic acid, are considered one of the key driving factors between the differences in community structure in the Southern Ocean (Nelson and Treguer, 1992). TOxN (and PO₄ by association) was identified in the BEST test as an important factor in the variability of phytoplankton distribution, but did not significantly correlate with the four dominant phytoplankton species (Fig. 4) contributing over 50% to changes in species composition in the GCB.

Nitrate drawdown by Southern Ocean diatoms is limited by dissolved iron (dFe) availability south of the STF (Sedwick et al., 2002), which may explain the dominance of the nanoplankton (with lower dFe and macronutrient requirements; Ho et al., 2003) in this study as they are not affected by low dFe concentrations as severely as the microplankton. The low silicic acid concentrations in the region between the SAF and the PF indicate that there was sufficient dFe to allow silicification and diatom growth, but either one or both of the macronutrients were then depleted to limiting concentrations (Assmy et al., 2013). As an essential nutrient for diatoms, silicic acid concentrations less than 2 $\mu\text{mol Si L}^{-1}$ were most common in the GCB, a level which is considered limiting for most diatom species (Paasche, 1973a & b; Egge and Asknes, 1992). However, even at stations with greater than 5 $\mu\text{mol Si L}^{-1}$, the small diatom species (<10 μm) were still dominant and represented over 40% of the total coccolithophore and diatom assemblage (numerically). There was a significant positive correlation between



silicic acid and the small ($<5 \mu\text{m}$) diatom *F. nana* (Pearson's product moment correlation = 0.986, $p < 0.05$, $n = 4$), although *F. nana* is likely to have a low cellular silicate requirement similar to *F. pseudonana* (Poulton et al., 2013) relative to larger diatom species, so the high abundance of *F. nana* in the high silicic acid waters could be indicative of a seasonal progression rather than silicic acid dependence. *Fragilariopsis* sp. have been observed at high abundances near the Ross Sea ice shelf (Grigorov and Rigual-Hernandez, 2014) and high abundances of large diatoms in the silicic acid- (and dFe-) replete waters may have been found further south than the sampling strategy of this study allowed. In the South Atlantic and the South Pacific Ocean silicic acid depletion moves southwards as spring to summer progresses, with a maximum diatom biomass observed in late January at 65°S (Sigmon et al., 2002; Le Moigne et al., 2013).

A significant negative correlation between *E. huxleyi* and silicic acid (Pearson's product moment correlation = -0.410, $p < 0.05$, $n = 24$) was found in this study, as has also been identified in the Scotia Sea (Hinz et al., 2012) and Patagonian Shelf (Balch et al., 2014). Low silicic acid may be considered a positive selection pressure for coccolithophores (Holligan et al. 2010), especially when other macronutrients (and dFe) are replete. However, non-blooming coccolithophore species are now recognized as having silicic acid requirements, though this requirement is conspicuously absent from *E. huxleyi* (Durak et al., 2016). Therefore the positive selection pressure at low silicic acid concentrations in the GCB is likely to be *E. huxleyi* specific rather than a coccolithophore-wide phenomena. To the south of the PF silicic acid increased (from < 1 to $> 3 \mu\text{mol Si L}^{-1}$) with five stations between the SAF and PF (and one south of the PF, station GCB1-59), all numerically dominated by *E. huxleyi*, while other stations to the south of the PF were dominated by diatoms (Fig. 2).

These results from the GCB indicate a progression of mineralizing phytoplankton southwards during spring as irradiance conditions become optimal and macronutrients are depleted. Low silicic acid is often associated with a high residual nitrate concentrations (defined as $[\text{NO}_3^-] - [\text{Si}(\text{OH})_4]$), as has been observed on the Patagonian Shelf (Balch et al., 2014). The highest coccolithophore abundances in this study (excluding the Patagonian Shelf) were indeed observed in regions with 'residual nitrate' concentrations greater than $10 \mu\text{mol NO}_3 \text{ L}^{-1}$ (Balch et al., 2016). As silicic acid is depleted in the more northerly surface waters in spring, diatoms progressively become more successful further south as irradiance conditions allow, thereby producing a large HNLSiLC area between the Sub-Antarctic Front and Polar Front; an ideal environment for late summer *E. huxleyi* dominated communities to develop (Figure 6).

Dissolved iron is recognized as a strong control on phytoplankton growth, community composition and species biogeography (e.g., Boyd, 2002, Boyd et al., 2015). In this study, dFe measurements were only made at a small number of sampling stations ($n = 6$; Twining, unpublished data, Balch et al., 2016) limiting their use in the multivariate statistical analysis of community composition. For these stations dFe showed a statistically significant negative correlation (Pearson's product moment = -0.957, $p < 0.01$) with PC2 from the environmental analysis (Fig. S2). PC2 described the environmental variables least related to latitude (pH, $p\text{CO}_2$ and \bar{E}_{MLD}), indicating that dFe was also decoupled from the strong latitudinal gradient in the environmental parameters (i.e. SST, Ω_{calcite} , macronutrients) in the GCB in the austral spring/summer.



Interestingly, dFe concentrations did positively correlate with coccolithophore abundance (Pearson's product moment correlation = 0.858, $p < 0.05$) rather than diatom abundance ($p = 0.132$, ns) (Fig. S2). Overall, these data support the hypothesis that coccolithophores occupy a niche unoccupied by large diatoms when dFe is replete and silicic acid is depleted (Balch et al., 2014; Hopkins et al., 2015). The numerical dominance of small diatoms less than 20 μm in the GCB during austral spring and summer, alongside the coccolithophore *E. huxleyi*, is thus potentially due to the reduced impact of nutrient limitation (dFe, silicic acid) on small cells with high ratios of surface area to volume (e.g., Hinz et al., 2012; Balch et al., 2014).

4.4 Relating the Great Calcite Belt to carbonate chemistry

Relating carbonate chemistry to phytoplankton distribution, growth and physiology is an important step when considering the potential effects of climate change and ocean acidification on marine biogeochemistry. In this study, no significant correlation (Spearman's $r = 0.259$, $p = 0.164$, $n = 27$) occurred between pH and Chl *a*. The inclusion of $p\text{CO}_2$ and Ω_{calcite} as influential factors in describing the GCB biogeography highlights the importance of understanding phytoplankton responses to carbonate chemistry as a whole rather than as individual carbonate chemistry parameters (Bach et al., 2015). Of the four major species driving the differences in mineralizing plankton community composition and biogeography across the GCB, only *F. pseudonana* abundance was positively correlated with $p\text{CO}_2$ (Pearson's product moment coefficient = 0.577, $p < 0.05$, $n = 16$).

The response of diatoms to increasing $p\text{CO}_2$ is not straight forward (e.g., Boyd et al., 2015), with some studies implying that large diatoms may be more successful in future climate scenarios (e.g., Tortell et al., 2008; Flynn et al., 2012), although changes in nutrient and light availability (via stronger stratification) may prevent a permanent switch in phytoplankton community structure (Bopp, 2005). The carbonate chemistry system is complex as biological activity also impacts on the concentration of each of the components. Organic matter production reduces dissolved inorganic carbon (C_T) and hence $p\text{CO}_2$ via photosynthesis, as well as increasing alkalinity (A_T) through nutrient uptake, while subsequent respiration and remineralisation of organic matter has the opposite impact. The simultaneous actions of biological and physical processes result in seasonal and localized changes in the carbonate system, which are often difficult to decouple.

In our study, there was no significant correlation between *E. huxleyi* and Ω_{calcite} (Pearson's product moment = 0.093), which may be viewed as somewhat surprising given the potential detrimental effects on calcifiers at low saturation states (e.g. Riebesell et al., 2000). However, the waters of the GCB remained oversaturated ($\Omega_{\text{calcite}} > 2$) throughout, and furthermore the relationship between coccolithophores, calcification and carbonate chemistry is now recognized as being complex and non-linear (e.g., Beaufort et al., 2011; Smith et al., 2012; Poulton et al., 2014; Rivero-Calle et al., 2015; Bach et al., 2015; Charalampopoulou et al., 2016; Marañón et al., 2016). Hence, significant gaps remain in our understanding of the *in situ* coccolithophore response to increasing $p\text{CO}_2$, reduced pH or decreasing Ω_{calcite} . Notably, a significant positive correlation



between *Pseudonitzschia* sp. and Ω_{calcite} also existed (Pearson's product moment correlation = 0.5924, $p < 0.01$, $n = 19$) across the GCB despite there being presently no known detrimental effect on diatoms of low saturation states. However, due to the tight coupling of temperature and Ω_{calcite} , the correlation is more likely to be temperature driven.

5 Summary

5 This study of the GCB further highlights the importance of understanding the environmental controls on the distribution of mineralizing nanoplankton in the Southern Ocean. The results of this study suggest that four nanoplankton (<20 μm) phytoplankton species (three diatoms and one coccolithophore; *F. pseudonana*, *F. nana*, *Pseudonitzschia* sp., and *Emiliania huxleyi*) numerically dominated the compositional variation in mineralizing phytoplankton biogeography across the GCB. The contribution of *E. huxleyi* to phytoplankton biomass (as measured by Chlorophyll *a*) was generally less than 5%,
10 although it increased up to 20% in association with high reflectance PIC features found on the Patagonian Shelf, north of South Georgia in the South Atlantic Ocean, and north of the Crozet Islands in the South Indian Ocean. This indicates that in the non-bloom conditions of the GCB, *E. huxleyi* could be as important as diatoms for phytoplankton biomass and primary production at localized spatial scales.

15 Latitudinal gradients in temperature, macronutrients and carbonate chemistry 'best' describe the variation of phytoplankton community composition in this study. However, not all species were directly sensitive to the same environmental gradients as determined to be influencing the overall biogeography. The negative correlation between *E. huxleyi* and silicic acid highlights the potential for a seasonal southward movement of *E. huxleyi* once diatom blooms have depleted silicic acid.

20 These results highlight that the Southern Ocean is highly dynamic system and further studies examining environmental controls on community distribution earlier in the productive season would greatly enhance overall understanding of the progression of phytoplankton community biogeography. The phytoplankton dynamics of the GCB are also more complex than first considered, with the nanophytoplankton (e.g., *F. pseudonana*) numerically dominant in non-bloom conditions (as opposed to microphytoplankton), which has further implications for modelling carbon export and projecting phytoplankton changes in future oceanic scenarios.



Competing interests

The authors declare that they have no conflict of interest.

Acknowledgements

We would like to thank all the scientists, officers and crew on board the *R/V Melville* and *R/V Revelle*, and Matt Durham
5 (Scripps Institution of Oceanography) in particular. Nutrient and salinity data are presented courtesy of the Oceanographic
Data Facility, Scripps Institute of Oceanography (ODF/SIO), with thanks to shipboard techs Melissa Miller and John
Calderwood. The GCB cruises were supported by the National Science Foundation (OCE-0961660 to WMB and BST., OCE-
0728582 to WMB., OCE-0961414 to NRB) and National Aeronautical and Space Administration (NNX11AO72G,
NNX11AL93G, NNX14AQ41G, NNX14AQ43A, NNX14AL92G, and NNX14AM77G to W.M.B.). HEKS and AJP were
10 supported by the Natural Environmental Research Council, including a NERC Fellowship to AJP (NE/F015054/1) and the
UK Ocean Acidification Research Program (NE/H017097/1) with a tied studentship to HEKS and an added value award to
AJP.

15 References

- Armand, L. K., Cornet-Barthaux, V., Mosseri, J. and Quéguiner, B.: Late summer diatom biomass and community structure
on and around the naturally iron-fertilised Kerguelen Plateau in the Southern Ocean, *Deep Sea-Res. Pt II*, 55(5–7), 653–676,
doi:10.1016/j.dsr2.2007.12.031, 2008.
- Arrigo, K. R., Worthen, D., Schnell, A. and Lizotte, M. P.: Primary production in Southern Ocean waters, *J. Geophys. Res.*,
20 103(C8), 15,1587–15,600, 1998.
- Assmy, P., Smetacek, V., Montresor, M., Klaas, C., Henjes, J., Strass, V. H., Arrieta, J. M., Bathmann, U., Berg, G. M.,
Breitbarth, E., Cisewski, B., Friedrichs, L., Fuchs, N., Herndl, G. J., Jansen, S., Krägfesky, S., Latasa, M., Peeken, I.,
Röttgers, R., Scharek, R., Schüller, S. E., Steigenberger, S., Webb, A. and Wolf-Gladrow, D.: Thick-shelled, grazer-
protected diatoms decouple ocean carbon and silicon cycles in the iron-limited Antarctic Circumpolar Current., *P. Natl.*
25 *Acad. Sci. USA.*, 110(51), 20633–8, doi:10.1073/pnas.1309345110, 2013.
- Bach, L. T., Riebesell, U., Gutowska, M. A., Federwisch, L., and Schulz, K. G.: A unifying concept of coccolithophore
sensitivity to changing carbonate chemistry embedded in an ecological framework, *Prog. Oceanogr.*, 135, 125–138, 2015
- Baines, S. B., Twining, B. S., Brzezinski, M. A., Nelson, D. M. and Fisher, N. S.: Causes and biogeochemical implications
of regional differences in silicification of marine diatoms, *Global Biogeochem. Cy.*, 24, 1–15, doi:10.1029/2010GB003856,
30 2010.



- Balch, W. M., Gordon, H. R., Bowler, B. C., Drapeau, D. T. and Booth E. S.: Calcium carbonate measurements in the surface global ocean based on Moderate-Resolution Imaging Spectroradiometer data. *J. Geophys. Res., Oceans* **110** (C7): C07001, 2005
- Balch, W. M., Bowler, B. C., Drapeau, D. T., Poulton, A. J. and Holligan, P. M.: Biominerals and the vertical flux of particulate organic carbon from the surface ocean, *Geophys. Res. Lett.*, 37(July), 1–6, doi:10.1029/2010GL044640, 2010.
- 5 Balch, W. M., Drapeau, D. T., Bowler, B. C., Lyczkowski, E., Booth, E. S. and Alley, D.: The contribution of coccolithophores to the optical and inorganic carbon budgets during the Southern Ocean Gas Exchange Experiment: New evidence in support of the ‘Great Calcite Belt’; hypothesis, *J. Geophys. Res.*, 116, C00F06, doi:10.1029/2011JC006941, 2011.
- 10 Balch, W. M., Drapeau, D. T., Bowler, B. C., Lyczkowski, E. R., Lubelczyk, L. C., Painter, S. C. and Poulton, A. J.: Surface biological, chemical, and optical properties of the Patagonian Shelf coccolithophore bloom, the brightest waters of the Great Calcite Belt, *Limnol. Oceanogr.*, 59(5), 1715–1732, doi:10.4319/lo.2014.59.5.1715, 2014.
- Balch, W. M., Bates, N. R., Lam, P. J., Twining, B. S., Rosengard, S. Z., Bowler, B. C., Drapeau, D. T., Garley, R., Lubelczyk, L. C., Mitchell, C. and Rauschenberg, S.: Factors regulating the Great Calcite Belt in the Southern Ocean and its biogeochemical significance, *Global Biogeochem. Cy.*, 30(8), 1124–1144, doi:10.1002/2016GB005414, 2016.
- 15 Barber, R. T. and Hiscock, M. R.: A rising tide lifts all phytoplankton: Growth response of other phytoplankton taxa in diatom-dominated blooms, *Global Biogeochem. Cy.*, 20(4), GB4S03, doi:10.1029/2006GB002726, 2006.
- Bates, N. R., Michaels, A. F. and Knap, A. H.: Seasonal and interannual variability of oceanic carbon dioxide species at US JGOFS Bermuda Atlantic Time-series Study (BATS) site, *Deep-Sea Res. Pt II*, 43, 347–383, 1996.
- 20 Bates, N. R., Best, M. H., Neely, K., Garley, R., Dickson, A. G., and Johnson, R. J.: Indicators of anthropogenic carbon dioxide uptake and ocean acidification in the North Atlantic Ocean. *Biogeosciences*, 9, 2509–2522, doi: 10.10519/bg-9-2509-2012, 2012
- Bathmann, U., Scharek, R., Klaas, C., Dubischar, C. and Smetacek, V.: Spring development of phytoplankton biomass and composition in major water masses of the Atlantic sector of the Southern Ocean, *Deep-Sea Res. Pt II*, 44(1–2), 51–67, 1997.
- 25 Beaufort, L., Probert, I., de Garidel-Thoron, T., Bendif, E. M., Ruiz-Pino, D., Metzl, N., Goyet, C., Buchet, N., Coupel, P., Grelaud, M., Rost, B., Rickaby, R. E. M. and de Vargas, C.: Sensitivity of coccolithophores to carbonate chemistry and ocean acidification, *Nature*, 476(7358), 80–8, doi:10.1038/nature10295, 2011.
- Belkin, I. M. and Gordon, A. L.: Southern Ocean fronts from the Greenwich meridian to Tasmania, *J. Geophys. Res.*, 101, 3675–3696, doi:10.1029/95JC02750, 1996.
- 30 Bopp, L.: Response of diatoms distribution to global warming and potential implications: A global model study. *Geophys. Res. Lett.* **32**: L19606, 2005
- Boyd, P. W.: Environmental factors controlling phytoplankton processes in the Southern Ocean, *J. Phycol.*, 38, 844–861, 2002.



- Boyd, P. W. and Newton, P. P.: Does planktonic community structure determine downward particulate organic carbon flux in different oceanic provinces? *Deep-Sea Res. Pt I*, 46(1), 63–91, doi:10.1016/S0967-0637(98)00066-1, 1999.
- Boyd, P. W., Strzepek, R., Fu, F. and Hutchins, D. A.: Environmental control of open-ocean phytoplankton groups: Now and in the future, *Limnol. Oceanogr.*, 55(3), 1353–1376, doi:10.4319/lo.2010.55.3.1353, 2010.
- 5 Boyd, P. W., Lennartz, S. T., Glover, D. M. and Doney, S. C.: Biological ramifications of climate-change-mediated oceanic multi-stressors, *Nat. Clim. Change.*, 5(1), 71–79, doi:10.1038/NCLIMATE2441, 2015.
- Caldeira, K. and Wickett, M.: Anthropogenic carbon and ocean pH, *Nature*, 425: 365, 2003.
- Charalampopoulou, A., Poulton, A. J., Tyrrell, T. and Lucas, M. I.: Irradiance and pH affect coccolithophore community composition on a transect between the North Sea and the Arctic Ocean, *Mar. Ecol-Prog. Ser.*, 431, 25–43,
10 doi:10.3354/meps09140, 2011.
- Charalampopoulou, A., Poulton, A. J., Bakker, D. C. E., Stinchcombe, M., Lucas, M. I. and Tyrrell, T.: Environmental drivers of coccolithophore abundance and cellular calcification across Drake Passage (Southern Ocean), *Biogeosciences* 13, 5917–5935, doi:10.5194/bg-13-5917-5935, 2016.
- Clarke, K. R.: Non-parametric multivariate analyses of changes in community structure, *Aust. J. Ecol.*, (18), 117–143, 1993.
- 15 Clarke, K. R. and Gorley, R. N.: *PRIMER v6: user manual/tutorial*, PRIMER v6., PRIMER-E, Plymouth., 2006.
- Clarke, K. R. and Warwick, R. M.: *Change in Marine Communities: An Approach to Statistical Analysis and Interpretation*, second ed. PRIMER-E, Plymouth., 2001.
- Cook, S. S., Whittock, L., Wright, S. W. and Hallegraeff, G. M.: Photosynthetic pigment and genetic differences between two Southern Ocean morphotypes of *Emiliania huxleyi* (Haptophyta)1, *J. Phycol.*, 47(3), 615–626, doi:10.1111/j.1529-
20 8817.2011.00992.x, 2011.
- Cook, S. S., Jones, R. C., Vaillancourt, R. E. and Hallegraeff, G. M.: Genetic differentiation among Australian and Southern Ocean populations of the ubiquitous coccolithophore *Emiliania huxleyi* (Haptophyta), *Phycologia*, 52(4), 368–374, doi:10.2216/12, 2013.
- Cubillos, J., Wright, S., Nash, G., de Salas, M., Griffiths, B., Tilbrook, B., Poisson, A and Hallegraeff, G.: Calcification
25 morphotypes of the coccolithophorid *Emiliania huxleyi* in the Southern Ocean: changes in 2001 to 2006 compared to historical data, *Mar. Ecol-Prog. Ser.*, 348, 47–54, doi:10.3354/meps07058, 2007.
- de Baar, H. J. W., Boyd, P. W., Coale, K. H., Landry, M. R., Tsuda, A., Assmy, P., Bakker, D. C. E., Bozec, Y., Barber, R. T., Brzezinski, M. A., Buesseler, K. O., Boye, M., Croot, P., Gervais, F., Gorbunov, M., Harrison, P. J., Hiscock, W. T., Laan, P., Lancelot, C., Law, C. S., Levasseur, M., Marchetti, A., Millero, F. J., Nishioka, J., Nojirim, Y., van Oijen, T.,
30 Riebesell, U., Rijkenberg, M. J. A., Saito, H., Takeda, S., Timmermans, K. R., Veldhuis, M. J. W., Waite, A. M. and Wong, C. S.: Synthesis of iron fertilization experiments: From the Iron Age in the Age of Enlightenment, *J. Geophys. Res.*, 110(C9), C09S16, doi:10.1029/2004JC002601, 2005.
- Deppeler, S. L. and Davidson, A. T.: Southern Ocean phytoplankton in a changing climate, *Front. Mar. Sci.*, 4:40, doi:10.3389/fmars.2017.00040, 2017.



- Dickson, A. G. and Millero, F. J.: A comparison of the equilibrium constants for the dissociation of carbonic acid in seawater media., *Deep-Sea Res.*, 36, 1733–1743, 1987.
- Doney, S. C., Fabry, V. J., Feely, R. A and Kleypas, J. A: Ocean acidification: the other CO₂ problem., *Annu. Rev. Mar. Sci.*, 1, 169–92, doi:10.1146/annurev.marine.010908.163834, 2009.
- 5 Dugdale, R. C., Wilkerson, F. P. and Minas, H. J.: The role of a silicate pump in driving new production, *Deep-Sea Res. Pt I*, 42(5), 697–719, 1995.
- Durak, G. M., Taylor, A. R., Probert, I., de Vargas, C., Audic, S., Schroeder, D. C., Brownlee, C. and Wheeler, G. L.: A role for diatom-like silicon transporters in calcifying coccolithophores, *Nat. Commun.*, 7:10543, doi:10.1038/ncomms10543, 2015.
- 10 Egge, J. K. and Asknes, D. L.: Silicate as a regulating nutrient in phytoplankton competition, *Mar. Ecol-Prog. Ser.*, 83, 281–289, 1992.
- Eynaud, F., Giraudeau, J., Pichon, J.-J. and Pudsey, C. J.: Sea-surface distribution of coccolithophores, diatoms, silicoflagellates and dinoflagellates in the South Atlantic Ocean during the late austral summer 1995, *Deep-Sea Res. Pt I*, 46(3), 451–482, doi:10.1016/S0967-0637(98)00079-X, 1999.
- 15 Flynn, K. J. K., Blackford, J. J. C., Baird, M. E. M., Raven, J. A., Clark, D. R., Beardall, J., Brownlee, C., Fabian, H. and Wheeler, G. L.: Changes in pH at the exterior surface of plankton with ocean acidification, *Nat. Clim. Change.*, 2(7), 510–513 doi:10.1038/nclimate1489, 2012.
- Froneman, P. W., McQuaid, C. D. and Perissinotto, R.: Biogeographic structure of the microphytoplankton assemblages of the South Atlantic and Southern Ocean during austral summer, *J. Plankton Res.*, 17(9), 1791–1802, doi:10.1093/plankt/17.9.1791, 1995.
- 20 Froneman, P. W., Pakhomov, E. A. and Balarin, M. G.: Size-fractionated phytoplankton biomass, production and biogenic carbon flux in the eastern Atlantic sector of the Southern Ocean in late austral summer 1997-1998, *Deep-Sea Res. Pt II*, 51(22–24), 2715–2729, 2004.
- Gall, M. P., Boyd, P. W., Hall, J., Safi, K. A. and Chang, H.: Phytoplankton processes. Part 1: Community structure during the Southern Ocean Iron RElease Experiment (SOIREE), *Deep-Sea Res. Pt II*, 48, 2551–2570, 2001.
- 25 Garcia, C. A. E., Garcia, V. M. T., Dogliotti, A. I., Ferreira, A., Romero, S. I., Mannino, A., Souza, M. S. and Mata, M. M.: Environmental conditions and bio-optical signature of a coccolithophorid bloom in the Patagonian shelf, *J. Geophys. Res-Oceans.*, 116(3), 1–17, doi:10.1029/2010JC006595, 2011.
- Grigorov, I. and Rigual-Hernandez, A.: Settling fluxes of diatoms to the interior of the Antarctic circumpolar current along 30 170° W, *Deep-Sea Res. Pt I*, doi:10.1016/j.dsr.2014.07.008, 2014.
- Hasle, G. R. and Syvertsen, E. E.: Chapter 2 - Marine Diatoms, in *Marine Phytoplankton*, edited by C. R. Tomas, pp. 5–385, Academic Press, San Diego., 1997.
- Haxo, F. T.: Photosynthetic action spectrum of the coccolithophorid, *Emiliania huxleyi* (Haptophyceae): 19' hexanoyloxyfucoxanthin as antenna pigment, *J. Phycol.*, 21(2), 282–287, 1985.



- Hinz, D. J., Poulton, A. J., Nielsdóttir, M. C., Steigenberger, S., Korb, R. E., Achterberg, E. P. and Bibby, T. S.: Comparative seasonal biogeography of mineralising nannoplankton in the Scotia Sea: *Emiliania huxleyi*, *Fragilariopsis* spp. and *Tetraparma pelagica*, *Deep-Sea Res. Pt II*, 59–60, 57–66, doi: 10.1016/j.dsr2.2011.09.002, 2012.
- Ho, T., Quigg, A., Finkel, Z. V., Milligan, A. J., Wyman, K., Falkowski, P. G. and Morel, M. M.: The elemental composition of some marine phytoplankton, *J. Phycol.*, 1159, 1145–1159, 2003.
- Holligan, P., Fernández, E., Aiken, J., Balch, W. M., Boyd, P., Burkill, P. H., Finch, M., Groom, S. B., Malin, G., Muller, K., Purdie, D. A., Robinson, C., Trees, C. C., Turner, S. M. and van der Wal, P.: A biogeochemical study of the coccolithophore, *Emiliania huxleyi*, in the North Atlantic, *Global Biogeochem. Cy.*, 7(4), 879–900 doi:10.1029/93GB01731/full, 1993.
- Holligan, P. M., Charalampopoulou, A. and Hutson, R.: Seasonal distributions of the coccolithophore, *Emiliania huxleyi*, and of particulate inorganic carbon in surface waters of the Scotia Sea, *J. Marine Syst.*, 82(4), 195–205, 2010.
- Honjo, S., Francois, R., Manganini, S. and Dymond, J.: Particle fluxes to the interior of the Southern Ocean in the Western Pacific sector along 170W, *Deep-Sea Res.*, 47, 2000.
- Hopkins, J., Henson, S.A., Painter, S.C. Tyrrell, T. and Poulton, A.J.: Phenological characteristics of coccolithophore blooms, *Global Biogeochem. Cy.*, 29, 239-253 doi:10.1002/2014GB004919, 2015.
- Knap, A.H., Michaels, A., Close, A.R., Ducklow, H. and Dickson, A.G.: Protocols for the joint global ocean flux study (JGOFS) core measurements. JGOFS Repr IOC Man Guid No 29 UNESCO 1994. 1996; 19.
- Kopczynska, E. E., Weber, L. H. and El-Sayed, S. Z.: Phytoplankton species composition and abundance in the Indian Sector of the Antarctic Ocean, *Polar Biol.*, 6, 161–169, 1986.
- Kopczynska, E. E., Fiala, M. and Jeandel, C.: Annual and interannual variability in phytoplankton at a permanent station off Kerguelen Islands, Southern Ocean, *Polar Biol.*, 20(5), 342–351, doi:10.1007/s003000050312, 1998.
- Korb, R. E., Whitehouse, M. J., Atkinson, A. and Thorpe, S. E.: Magnitude and maintenance of the phytoplankton bloom at South Georgia: a naturally iron-replete environment, *Mar. Ecol-Prog. Ser.*, 368, 75–91, doi:10.3354/meps07525, 2008.
- Korb, R. E., Whitehouse, M. J., Gordon, M., Ward, P. and Poulton, A. J.: Summer microplankton community structure across the Scotia Sea: implications for biological carbon export, *Biogeosciences*, 7(1), 343–356, doi:10.5194/bg-7-343-2010, 2010.
- Korb, R. E., Whitehouse, M. J., Ward, P., Gordon, M., Venables, H. J. and Poulton, A. J.: Regional and seasonal differences in microplankton biomass, productivity, and structure across the Scotia Sea: Implications for the export of biogenic carbon, *Deep-Sea Res. Pt II*, 59–60, 67–77, doi: 10.1016/j.dsr2.2011.06.006, 2012.
- Langer, G., Geisen, M., Baumann, K.-H., Kläs, J., Riebesell, U., Thoms, S. and Young, J. R.: Species-specific responses of calcifying algae to changing seawater carbonate chemistry, *Geochem. Geophys. Geosys.*, 7(9), doi:10.1029/2005GC001227, 2006.
- Langer, G., Probert, I., Nehrke, G. and Ziveri, P.: The morphological response of *Emiliania huxleyi* to seawater carbonate chemistry changes: an inter-strain comparison, *J. Nannoplankton. Res.*, 32(1), 29–34, 2011.



- Leblanc, K., Hare, C. E., Boyd, P. W., Bruland, K. W., Sohst, B., Pickmere, S., Lohan, M. C., Buck, K., Ellwood, M. and Hutchins, D. A.: Fe and Zn effects on the Si cycle and diatom community structure in two contrasting high and low-silicate HNLC areas, *Deep-Sea Res. Pt I*, 52(10), 1842–1864, doi:10.1016/j.dsr.2005.06.005, 2005.
- Le Moigne, F. A. C., Sanders, R. J., Villa-Alfageme, M., Martin, A. P., Pabortsava, K., Planquette, H., Morris, P. J. and Thomalla, S. J.: On the proportion of ballast versus non-ballast associated carbon export in the surface ocean, *Geophys. Res. Lett.*, 39(15), L15610, doi:10.1029/2012GL052980, 2012.
- Le Moigne, F. A. C., Boye, M., Masson, A., Corvaisier, R., Grossteffan, E., Guéneugues, A. and Pondaven, P.: Description of the biogeochemical features of the subtropical south-eastern Atlantic and the Southern Ocean south of South Africa during the austral summer of the International Polar Year, *Biogeosciences*, 10(1), 281–295, doi:10.5194/bg-10-281-2013, 2013.
- Lewis, E., and Wallace, D. W. R.: Program Developed for CO₂ System Calculations Rep. ORNL/CDIAC-105, Carbon Dioxide Information Analysis Center, Oak Ridge National Laboratory, U.S. Department of Energy, Oak Ridge, Tennessee, 1998.
- Marañón, E., Balch, W.M., Cermeño, P., González, N., Sobrino, C., Fernández, A., Huete-Ortega, M., López-Sandoval, D.C., Delgado, M., Estrada, M., Álvarez, M, Fernández-Guallart, E, and Pelejero, C.: Coccolithophore calcification is independent of carbonate chemistry in the tropical ocean. *Limnol. Oceanogr.*, doi: 10.1002/lno.1029, 2016.
- Martin, J. H., Fitzwater, S. E. and Gordon, R. M.: Iron deficiency limits phytoplankton growth in Antarctic waters, *Global Biogeochem. Cy.*, 4(1), 5–12, doi:10.1029/GB004i001p00005, 1990.
- Mehrbach, C., Culberson, C. H., Hawley, J. E. and Pytkowicz, R. M.: Measurement of the apparent dissociation constants of carbonic acid in seawater at atmospheric pressure., *Limnol. Oceanogr.*, 18, 897–907, 1973.
- Mohan, R., Mergulhao, L. P., Guptha, M. V. S., Rajakumar, A., Thamban, M., AnilKumar, N., Sudhakar, M. and Ravindra, R.: Ecology of coccolithophores in the Indian sector of the Southern Ocean, *Mar. Micropaleontol.*, 67(1–2), 30–45, doi:10.1016/j.marmicro.2007.08.005, 2008.
- Moore, C. M., Hickman, A. E., Poulton, A. J., Seeyave, S. and Lucas, M. I.: Iron–light interactions during the CROZet natural iron bloom and EXport experiment (CROZEX): II—Taxonomic responses and elemental stoichiometry, *Deep-Sea Res. Pt II*, 54(18–20), 2066–2084, doi:10.1016/j.dsr2.2007.06.015, 2007.
- Nelson, D. and Treguer, P.: Role of silicon as a limiting nutrient to Antarctic diatoms: Evidence from kinetic studies in the Ross Sea ice-edge zone, *Mar. Ecol-Prog. Ser.*, 80, 255–264, 1992.
- Orsi, A. H., Whitworth, T. and Nowlin Jr, W. D.: On the meridional extent and fronts of the Antarctic Circumpolar Current, *Deep-Sea Res. PtI*, 42(5), 641-673, 1995.
- Paasche, E. Silicon and the ecology of marine planktonic diatoms. 1. *Thalassiosira pseudonana* (*Cyclotella nana*) grown in chemostats with silicate as the limiting nutrient. *Marine Biology* 19:117-126, 1973a.
- Paasche, E. Silicon and the ecology of marine plankton diatoms. II. Silicate-uptake kinetics in five diatom species. *Mar. Biol.*, 19:262-269, 1973b.



- Paasche, E. A review of the coccolithophorid *Emiliana huxleyi* (Prymnesiophyceae), with particular reference to growth, coccolith formation, and calcification-photosynthesis interactions. *Phycologia* 40: 503–529, 2001.
- Painter, S. C., Poulton, A. J., Allen, J. T., Pidcock, R. and Balch, W. M.: The COPAS08 expedition to the Patagonian Shelf: Physical and environmental conditions during the 2008 coccolithophore bloom, *Cont. Shelf Res.*, 30(18), 1907–1923, doi:10.1016/j.csr.2010.08.013, 2010.
- 5 Passow, U. and Carlson, C.: The biological pump in a high CO₂ world, *Mar. Ecol-Prog. Ser.*, 470(2), 249–271, doi:10.3354/meps09985, 2012.
- Petrou, K., Kranz, S. A., Trimborn, S., Hassler, C. S., Blanco, S., Sackett, O., Ralph, P. J. and Davidson, A. T.: Southern Ocean phytoplankton physiology in a changing climate, *J. Plant Physiol.*, 203, 135–150, doi:10.1016/j.jplph.2016.05.004, 10 2016.
- Pondaven, P., Ragueneau, O., Treguer, P., Hauvespre, A., Dezileau, L. and Reyss, J.: Resolving the “opal paradox” in the Southern Ocean, *Nature*, 405(6783), 168–72, doi:10.1038/35012046, 2000.
- Poulton, A. J., Sanders, R., Holligan, P. M., Stinchcombe, M. C., Adey, T. R., Brown, L. and Chamberlain, K.: Phytoplankton mineralization in the tropical and subtropical Atlantic Ocean, *Global Biogeochem. Cy.*, 20(4), GB4002, doi:10.1029/2006gb002712, 2006.
- 15 Poulton, A. J., Mark Moore, C., Seeyave, S., Lucas, M. I., Fielding, S. and Ward, P.: Phytoplankton community composition around the Crozet Plateau, with emphasis on diatoms and *Phaeocystis*, *Deep-Sea Res. Pt II*, 54(18–20), 2085–2105, doi:10.1016/j.dsr2.2007.06.005, 2007.
- Poulton, A. J., Charalampopoulou, A., Young, J. R., Tarran, G. A., Lucas, M. I. and Quartly, G. D.: Coccolithophore dynamics in non-bloom conditions during late summer in the central Iceland Basin (July–August 2007), *Limnol. Oceanogr.*, 20 55(4), 1601–1613, 2010.
- Poulton, A. J., Young, J. R., Bates, N. R. and Balch, W. M.: Biometry of detached *Emiliana huxleyi* coccoliths along the Patagonian Shelf, *Mar. Ecol-Prog. Ser.*, 443, 1–17, doi:10.3354/meps09445, 2011
- Poulton, A. J., Painter, S. C., Young, J. R., Bates, N. R., Bowler, B., Drapeau, D., Lyczsckowski, E. and Balch, W. M.: The 25 2008 *Emiliana huxleyi* bloom along the Patagonian Shelf: Ecology, biogeochemistry, and cellular calcification, *Global Biogeochem. Cy.*, 27(4), 1023–1033, doi:10.1002/2013GB004641, 2013.
- Poulton, A. J., Stinchcombe, M. C., Achterberg, E. P., Bakker, D. C. E., Dumousseaud, C., Lawson, H. E., Lee, G. A., Richier, S., Suggett, D. J. and Young, J. R.: Coccolithophores on the north-west European shelf: calcification rates and environmental controls, *Biogeosciences Discuss.*, 11(2), 2685–2733, doi:10.5194/bg-11-2685-2014, 2014.
- 30 Raven, J. A. and Geider, R. J.: Temperature and algal growth, *New Phytol.*, 110, 441–461, 1988.
- Read, J. F., Pollard, R. T. and Allen, J. T.: Sub-mesoscale structure and the development of an eddy in the Subantarctic Front north of the Crozet Islands, *Deep-Sea Res. Pt II*, 54(18–20), 1930–1948, doi:10.1016/j.dsr2.2007.06.013, 2007.
- Riebesell, U., Zondervan, I., Rost, B., Tortell, P., Zeebe, R. and Morel, F.: Reduced calcification of marine plankton in response to increased atmospheric CO₂, *Nature*, 407, 2–5, 2000.



- Rivero-Calle, S., Gnanadesikan, A., Del Castillo, C. E., Balch, W. M. and Guikema, S. D.: Multidecadal increase in North Atlantic coccolithophores and the potential role of rising CO₂, *Science*, 350 (6267), 1533–1537, 2015.
- Robbins, L. L., Hansen, M. E., Kleypas, J. A. and Meylan, S. C.: CO₂calc: A user-friendly seawater carbon calculator for Windows, Mac OS X, and iOS (iPhone)Rep., 17 pp, US Geological Survey, Reston, VA, USA, 2010.
- 5 Salter, I., Lampitt, R. S., Sanders, R., Poulton, A., Kemp, A. E. S., Boorman, B., Saw, K. and Pearce, R.: Estimating carbon, silica and diatom export from a naturally fertilised phytoplankton bloom in the Southern Ocean using PELAGRA: A novel drifting sediment trap, *Deep-Sea Res. Pt II*, 54(18–20), 2233–2259, 2007.
- Sarmiento, J. L., Hughes, T. M. C., Stouffer, R. J. and Manabe, S.: Simulated response of the ocean carbon cycle to anthropogenic climate warming, *Nature*, 393(May), 245–249, 1998.
- 10 Sarmiento, J. L., Slater, R., Barber, R., Bopp, L., Doney, S. C., Hirst, A. C., Kleypas, J., Matear, R., Mikolajewicz, U., Monfray, P., Soldatov, V., Spall, S. A. and Stouffer, R.: Response of ocean ecosystems to climate warming, *Global Biogeochem. Cy.*, 18(3), doi:10.1029/2003GB002134, 2004.
- Sarthou, G., Timmermans, K. R., Blain, S. and Treguer, P.: Growth physiology and fate of diatoms in the ocean: a review, *J. Sea Res.*, 53(1–2), 25–42, doi:10.1016/j.seares.2004.01.007, 2005.
- 15 Schmoker, C., Hernández-León, S., and Calbet, A.: Microzooplankton grazing in the oceans: impacts, data variability, knowledge gaps and future directions. *J. Plankton Res.*, 35(4), 691–706, 2013.
- Scott, F. J. and Marchant, J.: Antarctic Marine Protists, Australian Biological Resources Study, Canberra., 2005.
- Sedwick, P. ., Blain, S., Quéguiner, B., Griffiths, F. ., Fiala, M., Bucciarelli, E. and Denis, M.: Resource limitation of phytoplankton growth in the Crozet Basin, Subantarctic Southern Ocean, *Deep-Sea Res. Pt II*, 49(16), 3327–3349, doi:10.1016/S0967-0645(02)00086-3, 2002.
- 20 Sigmon, D. E., Nelson, D. M. and Brzezinski, M. A.: The Si cycle in the Pacific sector of the Southern Ocean: seasonal diatom production in the surface layer and export to the deep sea, *Deep-Sea Res. Pt II*, 49(9–10), 1747–1763, doi:10.1016/S0967-0645(02)00010-3, 2002.
- Signorini, S. R., Garcia, V. M. T., Piola, A. R., Garcia, C. A. E., Mata, M. M. and McClain, C. R.: Seasonal and interannual variability of calcite in the vicinity of the Patagonian shelf break (38°S–52°S), *Geophys. Res. Lett.*, 33(16), L16610, doi:10.1029/2006GL026592, 2006.
- 25 Smith, H. E. K.: The contribution of mineralising phytoplankton to the biological carbon pump in high latitudes. PhD, University of Southampton, 2014.
- Smith, H. E. K., Tyrrell, T., Charalampopoulou, A., Dumousseaud, C., Legge, O. J., Birchenough, S., Pettit, L. R., Garley, R., Hartman, S. E., Hartman, M. C., Sagoo, N., Daniels, C. J., Achterberg, E. P. and Hydes, D. J.: Predominance of heavily calcified coccolithophores at low CaCO₃ saturation during winter in the Bay of Biscay., *P. Natl. Acad. Sci. USA*, 109(23), 8845–9, doi:10.1073/pnas.1117508109, 2012.
- 30



Tortell, P. D., Payne, C. D., Li, Y., Trimborn, S., Rost, B., Smith, W. O., Riesselman, C., Dunbar, R. B., Sedwick, P. and DiTullio, G. R.: CO₂ sensitivity of Southern Ocean phytoplankton, *Geophys. Res. Lett.*, 35(4), 1–5, doi:10.1029/2007GL032583, 2008.

5 Tsuchiya, M., Talley, L. D. and McCartney, M. S.: Water-mass distributions in the western South Atlantic; A section from South Georgia Island (54S) northward across the equator, *J. Marine Sys.*, 52, 55–81, 1994.

Venables, H. and Moore, C. M.: Phytoplankton and light limitation in the Southern Ocean: Learning from high-nutrient, high-chlorophyll areas, *J. Geophys. Res.*, 115(C2), C02015, doi:10.1029/2009JC005361, 2010.

Verbeek, J. W.: Recent calcareous nannoplankton in the southernmost Atlantic, *Polarforschung*, 59(1/2), 45–60, 1989.

10 Winter, A., Jordan, R. W. and Roth, P. H.: Biogeography of living coccolithophores in ocean waters, in *Coccolithophores*, edited by A. Winter and W. G. Siesser, pp. 39–49, Cambridge University Press, Cambridge., 1994.

Winter, A., Henderiks, J., Beaufort, L., Rickaby, R. E. M. and Brown, C. W.: Poleward expansion of the coccolithophore *Emiliana huxleyi*, *J. Plankton Res.*, 0, 1–10, doi:10.1093/plankt/fbt110, 2013.

Young, J., Geisen, M., Cros, L., Kleijne, A., Sprengel, C., Probert, I. and Ostergaard, J.: A guide to extant coccolithophore taxonomy, *J. Nannoplankton Res.*, (Special Issue 1), 2003.

15



Tables

Table 1: Details of Great Calcite Belt sampling stations including station and cruise identifier; station position latitude (Lat) and Longitude (Long); sea surface temperature (SST); surface salinity (Sal); mixed layer average irradiance (\bar{E}_{MLD}); surface macronutrient concentrations (nitrate and nitrite, TOxN; phosphate, PO₄; silicate; ammonia, NH₄) surface carbonate chemistry parameters (normalized total alkalinity, A_T; dissolved inorganic carbon, C_T; pH; partial pressure of carbon dioxide (pCO_2); calcite saturation state ($\Omega_{calcite}$); and surface chlorophyll *a* (Chl *a*, mg m⁻³). Bold type indicates those used in the statistical analyses.

Table 2: Whole cell abundances of coccolithophores and diatoms in surface samples of the Great Calcite Belt, number of species in each group (S), Pielou's evenness (*J'*, **** denotes that *J'* was not calculated because only one species was present), the dominant species and its percentage contribution to the total numerical abundance of coccolithophores (%Co) or diatoms (%D). Holococcolithophores are abbreviated as Holococco*. Position denotes the location relative to the Southern Ocean fronts and zones (*Z*; north of the defined front) as defined by Orsi et al. (1995), letters after the front abbreviation denote specific locations and proximity to landmasses: Patagonian Shelf (PS); north of South Georgia (n SG); South Sandwich Islands (SS); Crozet Island (Cr), Kerguelen Island (K); Heard Island (H).

Table 3: Principal component (PC) scores, percentage variation described (%V) and the Pearson's product moment correlation associated with each variable and its significance level: **p < 0.0001*****, **p < 0.001****, **p < 0.005***, **p < 0.01**, p < 0.05.

Table 4: Phytoplankton assemblage groups identified, using the SIMPROF routine at p < 0.05, in the GCB (see also Figure 3), from the South Atlantic (GCB1) and the South Indian (GCB2) Oceans. Location is indicated as in Figure 2. Group Average Similarity (Group Av.Sim%) defines the percentage similarity of the community structure in all the stations within each group. The defining species contributing >50% to the species similarity for each group as identified through the SIMPER routine are presented alongside the average similarity for each species in each group (Average Similarity), where higher Similarity SD indicates more consistent contribution to similarity within the group. The percentage contribution per species to the group similarity (Contribution %) was also calculated.



Table 1

Station	Lat	Long	SST	Sal	\bar{E}_{MLD}	TOxN	PO ₄	Si(OH ₄)	NH ₄	A _T	C _T	pH	pCO ₂	Ω_{calc}	Chl <i>a</i>
	°S	°E	°C		mol PAR m ⁻² d ⁻¹		μmol L ⁻¹						μatm		mg m ⁻³
GCB1-6	51.79	-56.11	8.6	34.0	17.8	14.2	1.05	1.7	0.64	2336	2138	8.09	367	3.3	0.84
GCB1-16	46.26	-59.83	11.8	33.8	39.8	6.5	0.54	0.0	0.15	2333	2100	8.12	407	3.8	2.78
GCB1-25	45.67	-48.95	16.1	35.1	25.5	0.0	0.23	0.2	0.16	2320	2047	8.12	390	4.6	0.73
GCB1-32	40.95	-45.83	20.0	35.6	36.7	0.1	0.11	1.1	0.05	2307	2029	8.07	444	4.8	0.05
GCB1-46	42.21	-41.21	18.3	34.9	16.0	0.2	0.19	0.3	0.00	2328	2050	8.09	356	4.7	0.09
GCB1-59	51.36	-37.84	5.9	33.8	7.9	17.5	1.22	1.7	0.67	2368	2184	8.10	325	3.1	0.71
GCB1-70	59.25	-33.15	1.1	34.0	9.7	22.3	1.74	78.5	1.54	2388	2235	8.10	407	2.6	0.13
GCB1-77	57.28	-25.98	1.4	33.9	11.9	20.7	1.55	68.8	1.00	2386	2225	8.12	405	2.7	0.90
GCB1-85	53.65	-17.75	4.1	33.9	8.9	19.1	1.33	0.7	0.30	2369	2191	8.12	363	3.0	1.11
GCB1-92	50.4	-10.8	5.9	33.8	9.5	17.5	1.27	1.4	0.37	2362	2182	8.10	351	3.0	0.57
GCB1-101	46.31	-3.21	11.0	34.0	17.1	12.5	0.95	0.6	0.16	2345	2134	8.08	400	3.5	0.46
GCB1-109	42.63	3.34	15.1	34.4	20.0	5.3	0.56	0.8	0.00	2332	2098	8.07	359	4.0	0.39
GCB1-117	39.00	9.49	18.8	35.0	19.4	0.0	0.20	0.7	0.06	2321	2047	8.08	299	4.7	0.32
GCB2-5	37.09	39.48	21.0	35.5	11.2	0.0	0.05	1.1	0.07	2310	2005	8.10	340	5.2	0.12
GCB2-13	40.36	43.5	18.4	35.3	13.7	0.1	0.17	0.2	0.02	2307	2032	8.09	351	4.7	0.19
GCB2-27	45.82	51.05	7.7	33.7	5.8	20.1	1.35	2.9	0.14	2344	2194	8.00	425	2.6	0.47
GCB2-35	46.74	57.48	8.1	33.7	8.7	18.9	1.40	1.7	0.49	2363	2175	8.08	355	3.1	0.21
GCB2-43	47.52	64.04	6.5	33.7	5.9	21.7	1.53	0.5	0.38	2358	2197	8.04	387	2.8	0.34
GCB2-53	49.3	71.32	5.1	33.7	8.5	23.8	1.66	7.1	0.17	2359	2210	8.03	396	2.6	0.41
GCB2-63	54.4	74.56	3.5	33.8	3.0	25.3	1.70	10.5	0.21	2363	2210	8.07	360	2.6	0.26
GCB2-73	59.71	77.75	1.1	33.9	4.3	28.0	1.91	40.4	0.34	2372	2233	8.07	360	2.4	0.29
GCB2-87	54.25	88.14	3.4	33.9	4.3	24.2	1.69	9.0	0.45	2367	2216	8.06	367	2.6	0.28
GCB2-93	49.81	94.13	7.8	34.0	5.9	17.5	1.27	1.5	0.26	2345	2149	8.10	333	3.3	0.18
GCB2-100	44.62	100.5	13.0	34.8	4.7	6.4	0.55	0.2	0.15	2328	2083	8.11	326	4.1	0.33
GCB2-106	40.13	105.38	17.0	35.4	12.8	0.1	0.14	0.3	0.03	2318	2029	8.13	313	4.9	0.24
GCB2-112	40.26	109.6	15.8	34.9	11.1	3.6	0.43	0.2	0.00	2323	2060	8.11	332	4.4	0.36
GCB2-119	42.08	113.4	13.8	34.8	11.2	5.3	0.55	0.2	0.01	2320	2080	8.10	342	4.1	0.27



Table 2

Station	Position	Coccolithophores (Co)					Diatoms (D)				
		Cell mL ⁻¹	S	J'	Dominant species	% of Co	Cell mL ⁻¹	S	J'	Dominant species	% of D
GCB1-6	SAF, PS	242	1	****	<i>E. huxleyi</i>	100	125	10	0.89	<i>C. debilis</i>	26
GCB1-16	SAF, PS	1636	1	****	<i>E. huxleyi</i>	100	4589	2	0.21	<i>F. pseudonana</i>	96
GCB1-25	SAFZ	53	5	0.82	<i>S. mollischi</i>	38	25	7	0.87	<i>Pseudonitzschia</i> sp.	37
GCB1-32	STF	22	6	0.89	<i>U. tenuis</i>	31	15	3	0.79	<i>Nitzschia</i> sp.	55
GCB1-46	STF	3	1	****	Holococco*	100	2	1	****	<i>Chaetoceros</i> sp.	56
GCB1-59	sPF, n SG	565	1	****	<i>E. huxleyi</i>	100	164	14	0.78	<i>T. nitzschoides</i>	29
GCB1-70	sPF	103	1	****	<i>E. huxleyi</i>	100	700	8	0.36	<i>F. nana</i>	81
GCB1-77	sPF, SS	2	1	****	<i>E. huxleyi</i>	100	6787	1	****	<i>F. nana</i>	98
GCB1-85	sPF	28	1	****	<i>E. huxleyi</i>	100	139	15	0.86	<i>C. aequatorialis</i> sp.	22
GCB1-92	PFZ	77	2	0.13	<i>E. huxleyi</i>	98	102	14	0.8	<i>Pseudonitzschia</i> sp.	32
GCB1-101	SAFZ	91	5	0.64	<i>E. huxleyi</i>	68	50	6	0.66	<i>F. pseudonana</i>	59
GCB1-109	SAFZ	38	8	0.93	<i>E. huxleyi</i>	25	125	12	0.57	<i>Pseudonitzschia</i> sp.	61
GCB1-117	STF	13	4	0.95	<i>U. tenuis</i>	35	204	2	0.17	<i>C. closterium</i>	95
GCB2-5	STFZ	34	8	0.75	<i>E. huxleyi</i>	46	3	1	****	<i>Nanoneis hasleae</i>	47
GCB2-13	STFZ	46	8	0.65	<i>E. huxleyi</i>	57	25	3	0.7	<i>Nitzschia</i> sp.<20µm	67
GCB2-27	SAF, Cr	472	1	****	<i>E. huxleyi</i>	100	350	7	0.27	<i>F. pseudonana</i>	82
GCB2-36	SAF	164	4	0.43	<i>E. huxleyi</i>	83	146	15	0.79	<i>F. pseudonana</i>	33
GCB2-43	PFZ	11	1	****	<i>E. huxleyi</i>	100	83	11	0.63	<i>F. pseudonana</i>	54
GCB2-53	sPF, K	51	3	0.9	<i>E. huxleyi</i>	56	494	7	0.56	<i>F. pseudonana</i>	47
GCB2-63	sPF, H	132	1	****	<i>E. huxleyi</i>	100	245	9	0.46	<i>F. pseudonana</i>	71
GCB2-73	sPF	0	0	****	n/a	n/a	514	11	0.64	<i>F. pseudonana</i>	56
GCB2-87	sPF	106	1	****	<i>E. huxleyi</i>	100	172	8	0.73	<i>F. pseudonana</i>	42
GCB2-93	PFZ	98	4	0.49	<i>E. huxleyi</i>	80	71	14	0.77	<i>Pseudonitzschia</i> sp.	37
GCB2-100	SAFZ	121	6	0.31	<i>E. huxleyi</i>	87	155	8	0.55	<i>Pseudonitzschia</i> sp.	67
GCB2-106	STF	88	13	0.84	<i>E. huxleyi</i>	29	76	10	0.66	<i>Pseudonitzschia</i> sp.	54
GCB2-112	STF	120	6	0.41	<i>E. huxleyi</i>	80	242	9	0.43	<i>Pseudonitzschia</i> sp.	74
GCB2-119	SAFZ	117	8	0.35	<i>E. huxleyi</i>	82	63	8	0.64	<i>Pseudonitzschia</i> sp.	47



Table 3

Variable	PC1 - EV 5 (58%)		PC2 - EV 1.5 (17%)	
Temp	0.42	(0.97***)	0.08	(-0.10)
Salinity	0.36	(0.90***)	0	-
EML	0.24	(-0.55*)	0.5	(0.62**)
TOXN	-0.4	(-0.91***)	-0.05	(-0.06)
SIL	-0.35	(-0.77***)	0.02	(-0.03)
NH ₄	-0.35	(-0.81***)	-0.07	(-0.09)
pH	0.18	(-0.39)	-0.42	(-0.50*)
pCO ₂	-0.15	(-0.33)	0.75	(0.89***)
Ω _{calcite}	0.43	(-0.99***)	-0.02	(-0.02)

Table 4

Group	Station	Location	Group Av.Sim%	Defining Species	Average Similarity	Similarity SD	Contribution %
A	GCB1-46	STF	n/a	Holococco*	n/a	n/a	n/a
B	GCB1-117			<i>Cylindrotheca</i> sp.			
C	GCB1-70 GCB1-77	SBDY	54.5	<i>F. nana</i>	53.3	n/a	97.8
D	GCB1-25 GCB1-109 GCB2-36 GCB2-93 GCB2-100 GCB2-106 GCB2-112 GCB2-119	N of PF	47.6	<i>E. huxleyi</i> <i>Pseudonitzschia</i> sp.	13.9 12.7	2.68 3.6	29.3 26.7
E	GCB1-32 GCB1-101 GCB2-5 GCB2-13	N of SAF	42.3	<i>E. huxleyi</i> Holococco*	18.9 8.45	3.8 4.01	44.8 20
F	GCB1-6 GCB1-16 GCB1-59 GCB1-85 GCB1-92 GCB2-27 GCB2-43 GCB2-53 GCB2-63 GCB2-73 GCB2-87	PS S of SAF	40.6	<i>E. huxleyi</i> <i>F. pseudonana</i>	15.1 14.2	1.51 1.25	37.3 35



Figures

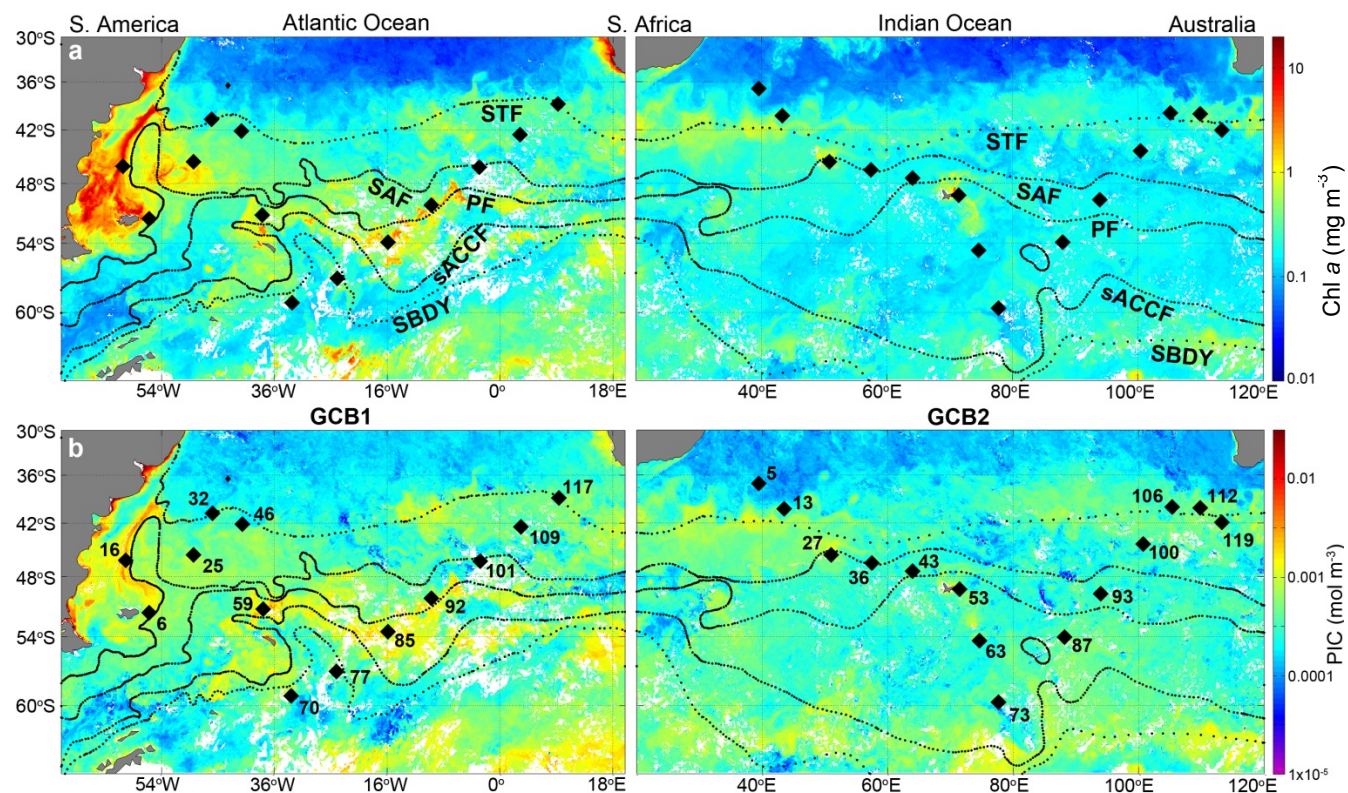


Figure 1 Rolling 32 day composite from MODIS-Aqua for both (a) Chlorophyll a (mg m^{-3}) and (b) PIC ($\mu\text{mol L}^{-1}$) for the South Atlantic sector (17th January to 17th February 2011) and the South Indian sector (18th February to 20th March 2012). Station number identifiers and averaged positions of fronts as defined by Orsi et al. (1995) are superimposed: Sub-tropical front (STF), Sub-Antarctic front (SAF), Polar Front (PF), Southern Antarctic Circumpolar Current Front (SACCF) and Southern Boundary (SBDY).

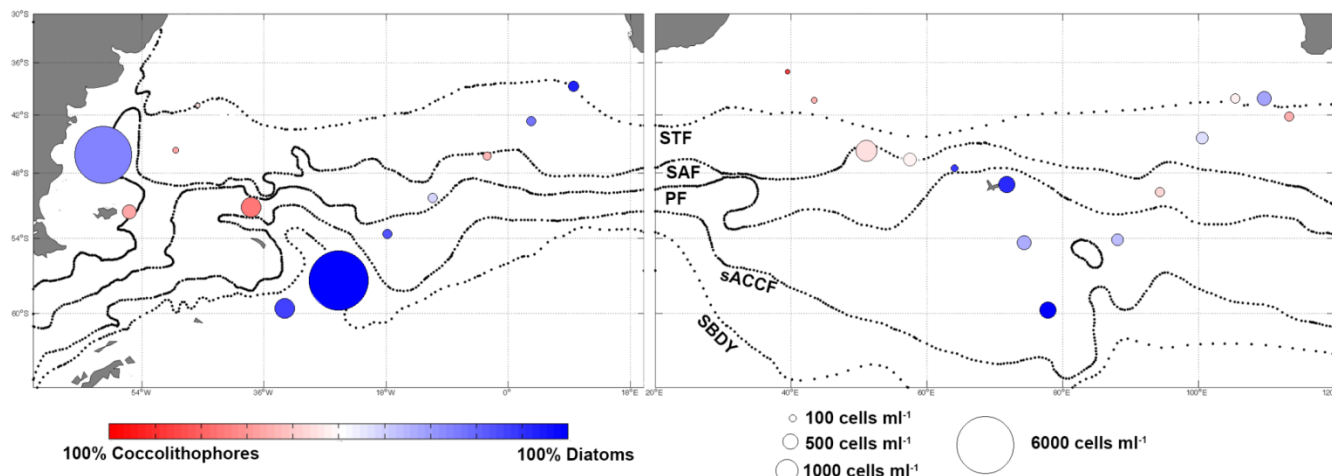
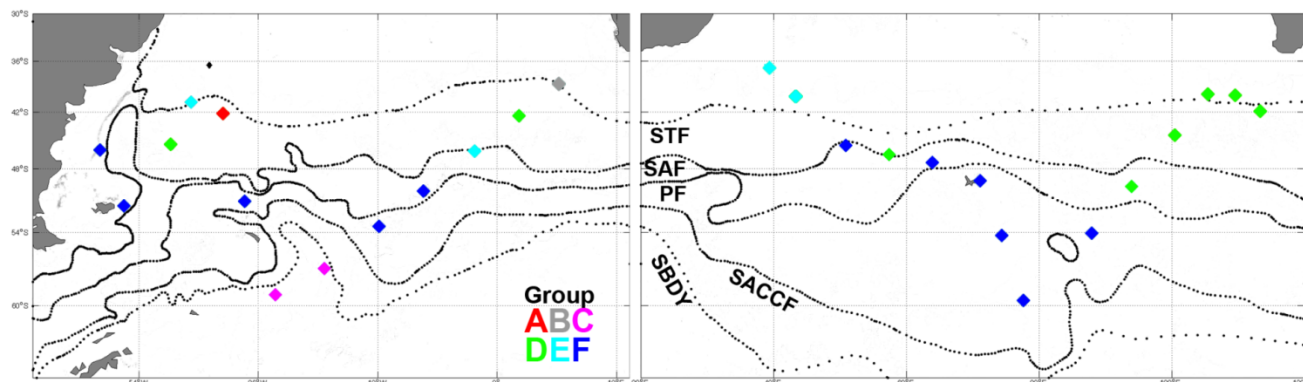


Figure 2 Coccolithophore and diatom abundance and dominance information. The area of the circles denotes abundance while shading denotes percentage contribution of each phytoplankton group, where red denotes coccolithophore dominance and blue denotes diatom dominance. Fronts are defined as in Figure 1



5

Figure 3 Statistically significant groups of coccolithophore and diatom communities in the Great Calcite Belt as identified by the SIMPROF routine. The colors designate which statistical group defines the coccolithophore and diatom assemblage at each station as shown in the group key. Fronts are defined as in Figure 1. See Table 4 for full group species descriptions.

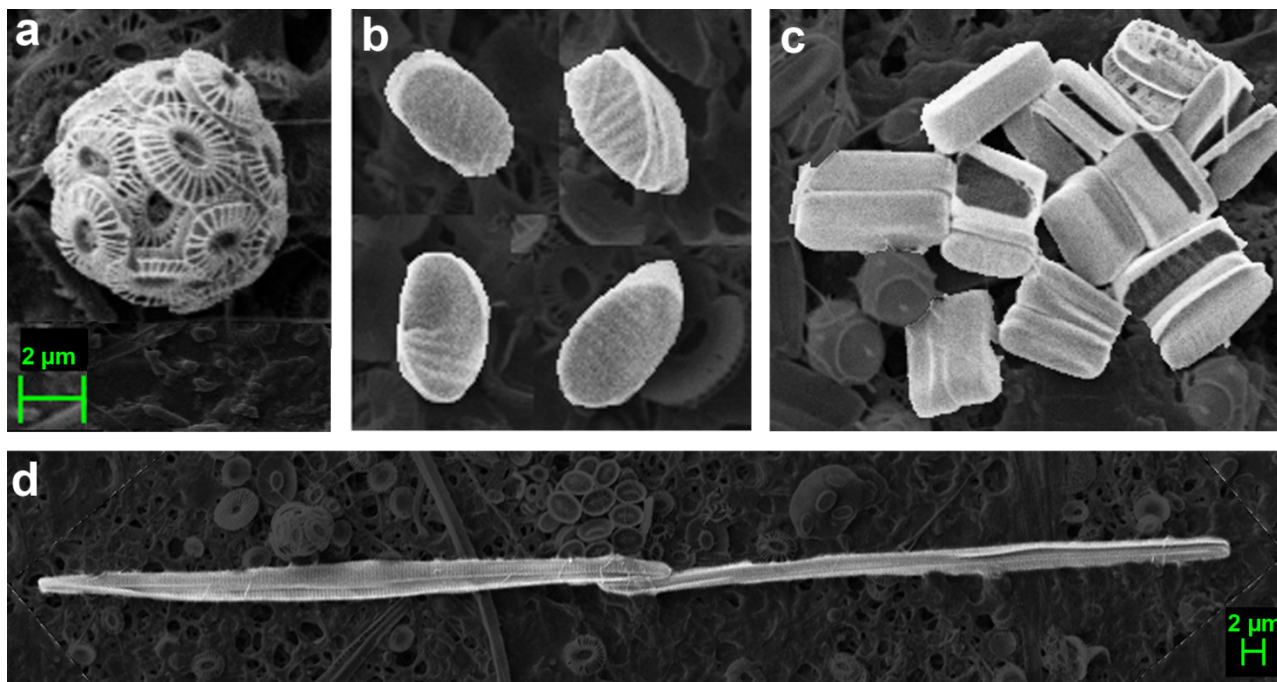


Figure 4 SEM images of the four phytoplankton species identified by the SIMPER analysis as characterizing the significantly different community structures. (a) *E. huxleyi*; (b) *F. pseudonana*; (c) *F. nana*; and (d): *Pseudonitzschia* sp.. Scale bar 2 μm for a-c and 5 μm for d.

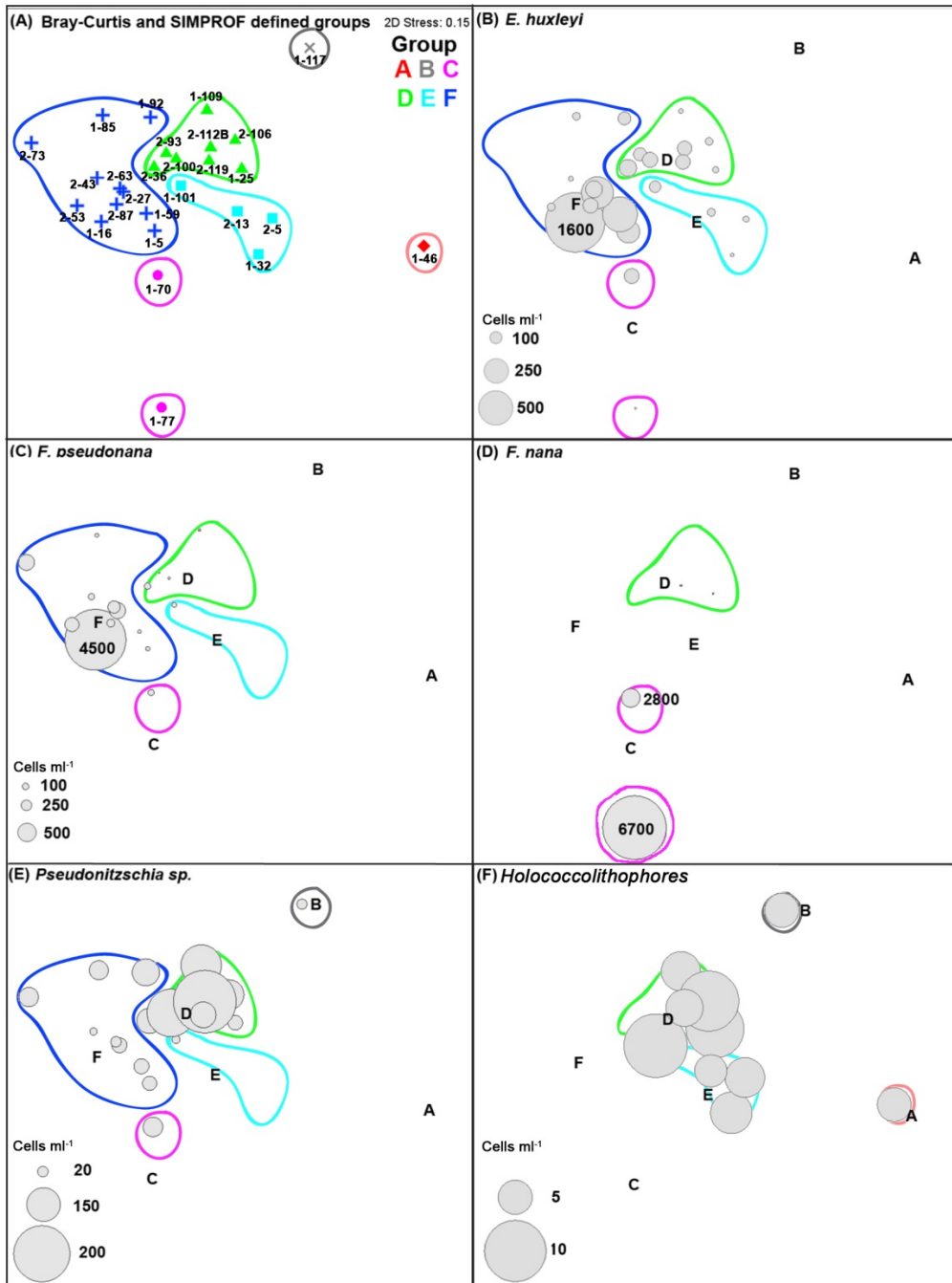


Figure 5 Two dimensional non-metric multidimensional scaling (nMDS) ordination of station groupings A) as defined by the SIMPROF routine, with group color identifiers as in Figure 3, where relative distances between the samples represent the similarity of species composition between phytoplankton communities. Overlay of bubble plots of the defining species abundance (cells mL⁻¹) characterizing the statistically significant groups in the GCB (see also Table 4; (B) *E. huxleyi* abundance; (C) *F. pseudonana* abundance; (D) *F. nana* abundance; (E) *Pseudonitzschia sp.* abundance; and (E) *Holococcolithophores* abundance). The two-dimensional stress of 0.15 gives a 'reasonable' representation of the data in a 2-D space (Clarke and Warwick, 2001).

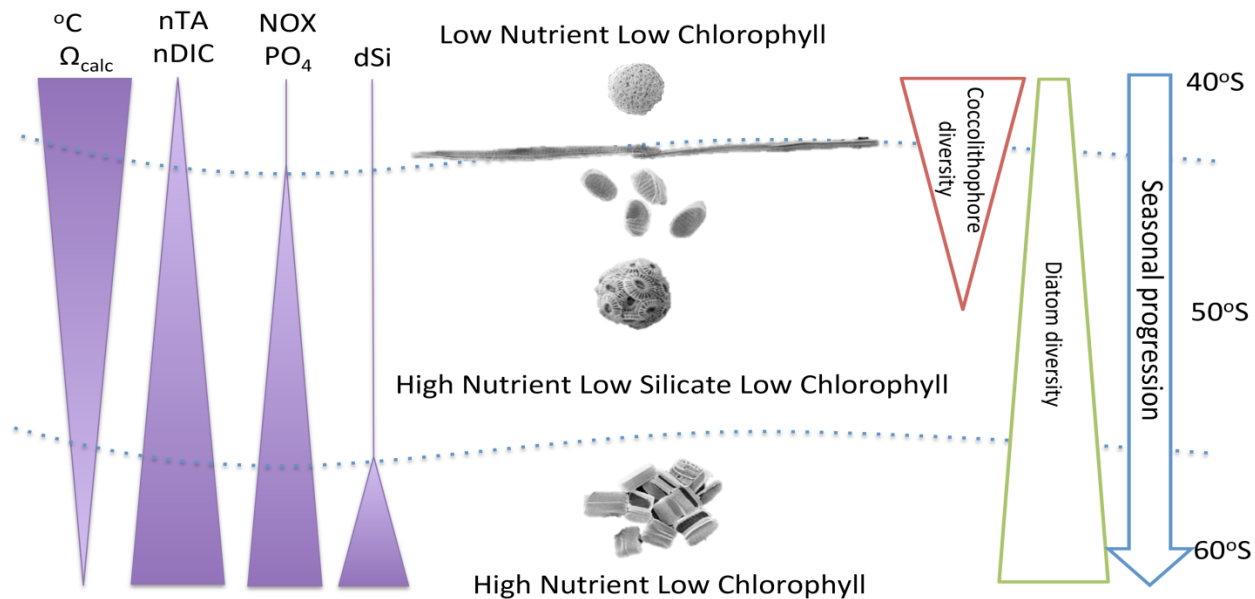


Figure 6 Schematic of the potential seasonal progression occurring in the Great Calcite Belt, allowing coccolithophores to develop after the main diatom bloom. Note phytoplankton example images are not to scale.